AJEMA GLOBAL RESEARCH NETWORK

AMERICAN Journal of Engineering, Mechanics and Architecture
Volume 4, Issue 06, 2026 ISSN (E): 2993-2637

A Dual-Method EES Framework for Temperature-Dependent Elastic Modulus Simulation and Material Selection in Five Metallic Alloys

Eman Mohamed Ismail
Department of Mechanical Engineering, Faculty of Engineering, University of Misan, Amarah, Iraq

Abstract: The paper describes a dual-method Engineering Equation Solver (EES) based simulation tool to calculate the temperature-dependent elastic moduli E(T) for five engineering metallic alloy-type materials: Copper C110, Ti-6Al-4V, Inconel 718, Hastelloy C276, and SS 316L from 20 °C to 600 °C. Two complementary computational techniques were developed and validated: Method A is based on using linear interpolation from experimental lookup tables published in the ASM Handbook, MMPDS-14, Haynes International, and MatWeb; Method B implements quadratic polynomial regression $E(T)=aT^2+bT+c$. Cross-validation of the two methods indicated a maximum deviation of 2.70% for all alloys and the entire thermal range, demonstrating good agreement between the two methods and high predictive accuracy of the polynomial equation model. The five alloys tested exhibited a monotonic decrease in elastic modulus with increasing temperature, with the average elastic modulus decreasing 21.3% at 600 °C when compared to the equivalent elastic moduli at ambient temperature. The alloy Inconel 718 exhibited the greatest relative elastic modulus retention, decreasing only 18.59% at 600 °C from ambient. The maximum thermal stress developed in alloy SS316L (1415 MPa at 600 °C) is primarily due to its relatively high coefficient of thermal expansion ($16x10^{-6}$/°C).

Results of the thermal sensitivity assessment resulted in the identification of two groups of metal alloys: one group having low sensitivity to temperature fluctuations (Cu C110 and Ti-6Al-4V, $|dE/dT| < 0.048$ GPa/°C) and a second group having high sensitivity to changes in temperature (Inconel 718, Hastelloy C276, and SS 316L, $|dE/dT| > 0.057$ GPa/°C). The development of an integrated multi-criteria methodology for evaluating metal alloys based on stiffness, retention loss, thermal sensitivity, and thermal stress produced a ranking of Inconel 718 > Hastelloy C276 > Ti-6Al-4V > Cu C110 > SS 316L, which has provided quantitative criteria that will allow for the selection of alloys that can be utilized in thermally demanding structural applications. The establishment of the dual-method EES process has simplified the entire thermal elastic response of each alloy into three scalar coefficients, which allows for the direct analytical incorporation of those three coefficients into finite element analysis equation solvers and digital twin platforms.

Keywords: Elastic Modulus, Temperature Dependence, EES Simulation, Polynomial Regression, Cross-Validation, Inconel 718, Hastelloy C276, Ti-6Al-4V, Material Selection, Thermal Stress.

1. Introduction

The Young's modulus or Elastic Modulus (E) is a basic material behaviour measure of how much resistance a given material can have to elastic deformation/external load. When performing structural engineering work (or any other) under thermal loading conditions, it is important to remember that Young's modulus, or elastic modulus, is not a constant material property but, rather, a temperature-dependent material property, which can exhibit progressive degradation with increased exposure to thermal conditions. This has substantial implications for the performance of engineering structures and their continued serviceability, overall construction durability, and overall structure length of time will not degrade when subjected to decreases in their physical integrity due to exposure to high temperature environments/as high temperature temperatures [1], [2].

The reason for elastic modulus reduction with temperature is the anharmonicity of the interatomic potentials. With a purely harmonic potential, the curvature of the energy well, which defines the elastic restoring force between atoms, will always remain the same temperature regardless of temperature change. However, real metallic solids have anharmonic contributions that will reduce the curvature as thermal energy increases the amplitude of atomic vibrations (i.e., they weaken the interatomic force constants) and cause a reduction in macroscopic stiffness [3]. The universal mechanism of bond weakening at higher temperatures occurs in all metallic alloys but can vary dramatically based on the alloy chemistry, crystal structure and microstructural strengthening mechanism; thus, there is a need for alloy compliant, or alloy specific, quantitative E(T) models validated against experimental reference data. Accurate forecasting of E(T) is very important for engineers designing a variety of components because E is used in multiple models to predict induced stress ($\sigma = E \cdot \alpha \cdot \Delta T$), thermal-induced deflection, and natural vibration frequencies all of which will change as the operating temperatures change over their service life. Additionally, when engineers input inaccurate values for E(T) into finite element analysis (FEA) models, those inaccuracies result in discrepancies being multiplied in stress fields and deformation calculations and can result in non-conservative assessments of the structural integrity [4]. Finally, the relative thermal stability of competitive alloys can be quantified using: E(T) retention values, thermal sensitivities (dE/dT), and the amount of thermal stress generated by the alloys which are the basis for selecting which of several alloys will be the most suitable for thermally demanding uses.

Increasingly, the conventional "trial and error" approach to alloy characterisation and property assessment is becoming constrained due to the high costs associated with performing experiments on the materials used in high-temperature applications [5], along with the relatively large size of the compositional and thermal parameter space needed for testing these materials at high temperatures. Typically, the temperature-dependent density of solid-metal materials is presented in the form of discrete, tabulated values in reference books (ASM Handbook[6], MMPDS-14 [7], etc.) or manufacturer data sheets (e.g., Haynes International [8] or MatWeb). However, corresponding analytical models which would allow the resulting values to be directly incorporated into computational simulation frameworks are either not provided or are still in the developmental process.

Over the last several years, there has been an increase in using data and computation to predict thermal and mechanical properties of materials. Many machine learning regression models (e.g., Gaussian process regression, neural networks, and symbolic regression) have shown effectiveness in predicting multiple mechanical properties simultaneously; they achieve this by taking advantage of the heteroscedasticity inherent in thermal datasets, while reducing the need for extensive experiments [9], [10]. Multi-fidelity datasets can be combined with physics-informed features that are well-established metallurgical concepts (e.g., atomic size mismatch and bulk modulus) in order to overcome the limitations of sparse experimental data [11], [12]. In addition, data-driven models combined with mechanistic domain knowledge can provide

quantitative relationships between microstructural variables and elastic constants over a broader range of thermal conditions [13], [14].

Simultaneously, high-throughput computation presents new avenues for the assessment of thermomechanical stability and screening of alloy compositions, allowing for a transition from expensive experimental iterative processes to rapid, data-driven methods of alloy discovery [15], [16], [17]. Specifically, the integration of physics-based models and computational frameworks has shown great benefit for interpreting the laws of material synthesis and properties for varied systems, such as austenitic stainless steels and nickel-based superalloys, as well as emerging refractory high-entropy alloys with better mechanical property characteristics in very high-temperature environments [18], [19], [20]

While there have been significant advancements in engineered systems for performing thermodynamic and heat transfer analyses on materials, the Engineering Equation Solver (EES) software, frequently used for those two functions, has been sporadically utilized to simulate materials with temperature-dependent, property-function performance phenomena. Accordingly, the relevant aspects of EES's use (or lack of use) had not been systematically investigated from the standpoint of temperature-dependent material property simulation and materials selection using a shared and validated framework. Furthermore, no published literature exists that offers a comparison and ranking of five highly critical industrial alloys via simultaneous modelling, validation, and ranking within a single computational environment. This study addresses both gaps; creating two distinct but correlated methodologies for establishing integrated empirical polynomial models and experimental data datafication of temperature-dependent elastic modulus characterisation for the five alloys examined herewith creating a direct, efficient, and easily understandable means for evaluating thermomechanical performance and selecting materials; readily usable in the design and engineering workflow [21], [22].

Although separate studies exist that quantify the high-temperature mechanical properties of four individual materials: Inconel 718 [23], Hastelloy C276 [24], SS 316L [25] and Ti-6Al-4V [26]; the development of a unified simulation framework that quantitatively models, cross-validates, and ranks all five alloys has yet to be accomplished. An additional new computational opportunity has not been pursued until now with regard to EES application towards temperature-dependent material property simulation using EES's parametric table automation, built in equation solving capability, and direct analytical differentiation, which this research explores.

The objectives of the paper are: 1) Create a dual-method EES-based simulation model to predict the elastic modulus at various temperatures (20-600 °C) for each of the five metal alloys. 2) Validate both methods and analyze inter-method deviations for all materials over the complete temperature range to establish the predictive accuracy of the polynomial method. 3) Compute and analyze four thermomechanical performance indicators (absolute elastic modulus E(T), retention loss, thermal sensitivity dE/dT, constrained thermal stress σ(T)) for each alloy over the entire temperature range. 4) Develop a weighted multi-criteria framework for material selection that uses all four mechanical performance indicators to provide a quantitative ranking of materials and guidance on material selection for structural engineering applications that will be subjected to elevated temperature loads.

2. Literature Review

Currently, the field of material science is going through a paradigm shift to the use of data-centric computational modelling frameworks that utilize high-throughput workflows and machine learning-assisted design to help overcome the challenges associated with traditional trial and error methods in the characterization of alloys [27], [28]. These advances are proving to be very useful in assisting with the high cost of conducting experiments and the vast search space for the composition of high-temperature alloys since much of the traditional resource-intensive characterization methods are becoming impractical for use in the high-temperature alloy development process. Recent academic work has focused on applying computational chemistry

and machine learning to the problem of predicting mechanical properties of complex metallic materials, through the use of deep surrogate models, Bayesian optimization techniques, and Gaussian process regressions for exploring and exploiting both low-characterized areas of the composition of interest and high-performing candidates [29], [30].

In the domain of physics-based and data-driven modeling, the establishment of quantitative relationships between microstructural variables and elastic constants is a currently important development Frameworks that use composition-based descriptors (such as atomic radius mismatch, bulk modulus, and temperature-dependent properties) were key to developing high-quality physics-based predictors for thermomechanical targets with very few experimental results [31], [32]. Thus, by combining fundamental mechanistic information from the domain with data-driven approaches, such an integrated approach will allow for rigorous identification of performance limits in high-temperature applications with materials that are sensitive to thermal changes due to degradation mechanisms.

The study of temperature influence on elastic modulus of metal alloys has been the subject of many years' worth of both theory and experimentation due to its key role in determining thermal stresses, deflection of structures, and dynamic mechanical behaviours of materials and components when subjected to thermal loading. Li et al. [33] have developed a physical basis for E(T) degradation based upon the anharmonic character of interatomic potentials via their formalisation of the empirical relationship associated with E(T) that has been shown to provide accurate predictions across FCC metals, BCC metals, and wrought superalloy systems through their second order polynomial fit to experimental data. The addition of temperature sensitive variables to calculations for E(T) has allowed for extrapolation of elastic modulus values beyond typical testing limits with respect to continuum mechanics, thereby addressing a crucial need for structural strength and reliability under extreme thermal conditions [34].

The discrete group of alloy systems studied here for purposes of high-temperature mechanical property characterization has been well documented to possess a known high-temperature mechanical property characterization. The precipitation-hardening characteristics of Inconel 718 are correlated with its temperature-dependent stiffness retention via the presence of coherent γ'/γ'' precipitates. The mechanisms responsible for contributing to the solid-solution strength of Hastelloy C276 are due in part to the Mo, W, and Cr solutes and these solutions provide the required mechanical integrity through a range of elevated temperatures, with long-term aging studies indicating that M_6C carbide precipitates begin to grow at the grain boundaries at temperatures in excess of 700 °. The elastic modulus evolution of SS 316L has been characterized using dynamic resonance measurements in accredited laboratories after exposure to an extended period of time at elevated temperatures, establishing the foundation for the experimental reference baseline used in the current study. For Ti-6Al-4V, modulus reduction caused by pre-transformational softening of the α-phase lattice is the predominant cause of modulus reduction below the α→β transus. Meanwhile, machine-learned (ML) models trained on austenitic stainless steel composition-property data have been validated as being able to predict the temperature-dependent elastic modulus of austenitic stainless steels from only the chemical composition of the materials, using first principles of thermodynamics.

As the paradigm of data-driven methodologies progresses, so too are new methods being developed to use computational simulations to evaluate material properties. The development of high-throughput computational workflows allowed for the integration of atomic-level data from microscopically small scales with macroscopic information derived from machine learning methods to facilitate quick screening of alloy compositions due to advances in computer science technologies [35], [36]. The successful application of hybrid architectures that combine generative models with high-quality first principles data has shown ample evidence for the potential of these methods to optimize alloys composed of multiple principal elements [37]. Collectively, these two different types of integrated methods illustrate how the development of

novel algorithms is critical to creating the linkage between localized atomistic simulations and the global predictive accuracy needed for optimizing alloys [38].

The Engineering Equation Solver (EES) platform has a demonstrated history of use for thermodynamic cycle analysis, heat transfer simulations, and parametric property assessment [Klein, 2023] within the computational domain. However, despite its computational functionalities, such as automation of parametric table generation, built-in equation solves, and analytical differentiate of regression models, EES has yet to be used systematically for the simulation of temperature-dependent material properties and multi-criteria selection between materials in a cross-validated manner. This void is addressed herein; the current research utilizes EES to create a dual-method simulation framework that will allow for the integration of physical fidelity associated with experimental data interpolation within physical models with the analytical efficiency associated with polynomial regression to provide a computationally efficient alternative to both traditional lookup tables and computationally intensive machine learning techniques for the five alloy systems studied.

To select quantitative materials for thermal applications, thermal and mechanical characteristics must be analysed as competing multiple performance criteria which makes it impossible to use single parameter rankings. Thermo-mechanical properties (absolute stiffness, dynamic elastic and component stress generation) of high-temperature structural alloys were benchmarked against the performance characteristics of nickel base superalloys in gas turbines, demonstrating the readiness of advanced material systems to transition to high mechanical performance in extreme thermal conditions. The integration of thermodynamic-informed ranking strategies has been essential to ensure predictive frameworks can reach physical truths of material high-temperature behaviour [39]. Additionally, the use of a weighted score matrix integrating the multiple thermo-mechanical indices as utilised by this work, provides a clear transparent repeatable and engineering aligned methodology for selecting alloys to compliment the more computationally intensive optimisation methods referenced in the literature [40].

There has been much research on how to characterize individual alloys, use machine learning to predict their properties, and design alloys computationally. However, there has never been a unified simulation framework based on EES that simultaneously implements, cross-validates, and compares temperature-dependent elastic modulus for all five alloys in this study, within a single parametric computational environment. The current study was done to fill this void by creating a dual method framework (Method A: interpolation Method B; polynomial regression) that combines the physical fidelity of data from reference handbooks with the analytical efficiency of closed-form polynomial expressions developed by systematic cross-validation, and applies these methods over a multi-criteria material selection analysis from 20 – 600 °C. The approach thus provides a computationally transparent, physically interpretable, and practically deployable extension of the machine-learning-intensive frameworks reported in much of the current materials science literature.

3. Methodology

3.1 Overview of the Engineering Equation Solver (EES) Platform

EES or Engineering Equation Solver is a non-linear iterative method developed by F-Chart Software that allows users to solve non-linear equations, determine engineering values quickly and provide results in a user-friendly format. EES is commonly used to analyze thermodynamic cycles as well as to develop models of heat transfer and simulate fluid mechanics. EES can solve many types of equations, including algebraic, differential, and integral equations, using a modified Newton-Raphson algorithm that utilizes automatic variable identification to automatically identify the inputs for the user. EES's Parametric Table function allows users to automatically generate iteratively defined variables over a user-specified range of parameters. The Lookup Table feature allows users to easily access experimental data using a fixed reference

or a variable keyword. EES's mathematical function capability enables the user to create and use polynomial regression formulas and their analytical derivative in an efficient manner.

EES has been selected as the study's simulation platform for three reasons. First, EES has the Parametric Table framework that allows for simultaneous evaluation of all five alloy models at 13 different temperature settings in a single solver run with results automatically propagated to all derived variables, including errors with cross-validation, thermal sensitivity, retention loss, and thermal stress, without the need for manual iterations to obtain results. Second, the algebraic transparency associated with EES equations provides a means to verify the computational implementation against the base mathematical formulations; thus, providing a complete and traceable record from the source data used to generate the regression coefficients to the simulation outputs. Lastly, EES establishes a means for direct analytical differentiation of polynomial expressions; therefore allowing for the closed-form computation of $dE/dT = 2aT + b$ to be performed as opposed to approximating using numerical finite-difference methodology. This capability has been directly utilized in the thermal sensitivity analysis as outlined in Section 3.4.

3.2 Dual-Method Framework Architecture

The dual-method framework for estimating energy (E) as a function of temperature (T) provides computationally independent pathways for obtaining E(T) predictions — called Method A (linear interpolation) and Method B (quadratic polynomial regression) — and are run simultaneously within the same EES environment over the temperature range of 20–600 °C, with 13 different points of evaluation: 20, 50, 100, 150, 200, 250, 300, 350, 400, 450, 500, 550, and 600 °C.

The purpose of using both methods at once is three-fold:

1. Independent prediction: Both methods will provide an independent prediction for E(T) based upon the same experimental data, but they will use different mathematical methods to make those predictions. Therefore, for every alloy and at every temperature point, two different predictions will be available.
2. (cross-validation): having both predicted outputs can be simultaneously evaluated against each other across every temperature data point (T) which provides a direct quantitative cross-validation evaluation between the polynomial output (E_B) to the experimental reference (E_A). Therefore, this cumulative cross-validation error profile (ε(T)) gives the capability of characterizing the accuracy of the polynomial model by comparing it back to the reference experimental baseline using the following equation $\varepsilon(T)=(|E\_B-E\_A|/E\_A)x100\%$.
3. Complete analytically complementary output: Method A maintains the physical fidelity to the experimental reference values by producing E(T) at discrete measured points while Method B is producing a continuous variable E(T) (which can also be analytically differentiated). Therefore, derivatives of E(T) with respect to temperature (dE/dT), retention losses and thermal stress values can be computed together from both methods with no need for interpolation. The combined output from both methods provides combined capability that neither output alone can produce.

Methodologically speaking, using both linear interpolation and polynomial regression (the two methods being used) is based upon using methods together that are complementary to each other. For example, although linear interpolation (Method A) is mathematically transparent and provides an exact reproduction of the experimental data at temperature of measurement (known as "raw" data in engineering terminology), it's widely used as a method of property retrieval, in engineering standards and FEA preprocessors. Linear interpolation provides no predictive capability between data points except on a piecewise linearity basis; it can't be differentiated analytically; and at runtime it requires the use of tabular data. Polynomial regression (Method B) overcomes these limitations: it provides a smooth continuous function of the relationship between temperature and other dependent variables (E(T)), has an analytical derivative of that function (dE/dT), and can be represented using three coefficients (i.e., it requires less storage

space). However, polynomial regression also adds error compared to the experimental data that used to fit the polynomial regression curve to the experimental data. By using both methods, the present methodology can be used to quantify the difference between the two methods through the use of cross-validation. This methodology provides a reference to physic-based models (through the use of linear interpolation) and a more computationally efficient analytical model (through the use of polynomial regression), along with a method of quantifying the errors associated with the analytical model.

3.3 Method A: Linear Interpolation from Experimental Lookup Tables

3.3.1 Experimental Data Sources

Reference data compiled under Method A for the elastic modulus is based on four authoritative sources widely accepted by the aerospace, nuclear, chemical processing, and materials engineering communities: ASM Handbook, Volume 2., which consists of non- ferrous alloys' properties including copper C110 and titanium Ti-6Al-4V, giving temperature dependent mechanical property data validated by standardised testing protocols. MMPDS-14 (Metallic Materials Properties Development and Standardization). includes certified mechanical property data for aerospace grade titanium Ti-6Al-4V and stainless steel SS-316L and is the most rigorously validated source of allowable mechanical property values for aerospace structural applications. Haynes International Technical Bulletins list high temperature elastic modulus data for Inconel 718 and Hastelloy C276 taken from the alloy manufacturers' certified property sheets and independently validated using corresponding test data. MatWeb Material Property Database provides supplementary comparative data for all five alloys to verify their consistency against those provided from the principal sources.

A total of 13 experimental E(T) data points for each alloy were gathered at 12 different temperatures (20, 50, 100, 150, 200, 250, 300, 350, 400, 450, 500 and 550 °C), resulting in the lookup table dataset for Method A; the complete dataset can be found in Table 1.

Table 1. Experimental elastic modulus E (GPa) — Method A lookup table (ASM Handbook, MMPDS-14, Haynes International, MatWeb).

T (°C)	Cu C110	Ti-6Al-4V	Inconel 718	Hastelloy C276	SS 316L
20	117	114	200	205	193
50	116	113	199	203	192
100	114	111	196	200	189
150	112	109	193	197	186
200	110	107	190	193	183
250	108	105	187	190	180
300	105	103	183	186	176
350	103	101	180	182	173
400	100	98	176	178	169
450	98	96	172	174	165
500	95	93	168	169	161
550	93	91	164	164	156
600	90	88	159	159	151

3.3.2 Linear Interpolation Procedure

In the EES environment, Method A uses piecewise linear interpolation to interpolate between neighbouring experimental data points. An elastic modulus value is calculated through linear interpolation at any evaluation temperature (denoted as T) that lies between 2 consecutive observed measurement points, T_i and T_{i+1}.

$$E_A(T) = E_A(T_i) + \frac{E_{(T_{i+1})} - E_{(T_i)}}{T_{i+1} - T_i} \times (T - T_i) \qquad (1)$$

where $E(T_i)$ and $E(T_{i+1})$ are the elastic moduli obtained from experiments at two temperature extremes. The built-in INTERPOLATE function in EES implements the linear interpolation by addressing five named first-sources into the lookup tables for copper (C110), titanium 6-aluminum 4-vanadium, nickel-chromium-iron (Inconel 718), nickel-chromium-molybdenum (Hastelloy C-276), and stainless steel 316L, all five of which contain the same thirteen-point experimental datasets. At the two thermal endpoints - T = 20°C and T = 600°C - Method A yields the exact experimental values, confirming the physical correctness of the thermal endpoints. There are three reasons that led to the decision to use linear interpolation for Method A: It is mathematically simple and allows for complete traceability back to source data; it reproduces the experiment results completely at the measurement temperatures ensuring no interpolation error at the measurement points; and it is universally valid as a retrieval technique for engineering standards, FEA pre-processors, and materials property databases so that it establishes physically based, independently verifiable baseline against which Method B can be cross-validated.

3.3.3 Validation of Method A

By construction, Method A is internally validated via a piecewise linear interpolation of empirical reference data from the ASM Handbook, MMPDS-14, and Haynes International, it directly reflects the current state-of-knowledge experimental baseline for each alloy. Rehmer provide independent validation of the compatibility of the Method A reference values, as their elastic modulus measurement results for Ti-6Al-4V, IN718, and AISI 316L via dynamic resonance in an accredited BAM laboratory are very reasonable relative to those found in this study, and therefore confirm the consistency of the experimental dataset throughout independent measuring agencies.

3.4 Method B: Quadratic Polynomial Regression

3.4.1 Model Formulation

Method B models the temperature-dependent elastic modulus as a second-order polynomial function of temperature:

$$E_{(T)} = aT^2 + bT + c \qquad (2)$$

T represents temperature in °C, E(T) denotes an elastic modulus measured in GPa, and the coefficients a, b, and c are specific to each alloy and were determined through a least squares fitting process using the 13 data points presented in Table 1. The justification for choosing a second order polynomial comes from three independent sources:

1) Theoretical Consistency: If consider the harmonic interatomic potential model, we can see how under certain assumptions (primarily at moderate temperatures) the elastic modulus will have a quadratic relationship as a function of temperature based on applying the interatomic potential energy to the second-order Taylor expansion about atomic displacement amplitude. Thus, this theoretical justification establishes the physical basis of the equation, which serves as a motivator for its polynomial form; or said another way, why one should not just use a random empirical formula for it.

2) Statistical parsimony: The three regression coefficients (a, b, c) give enough elasticity in their calculations to adequately model the curvature observed at each of the 13 data points in the dataset without over-fitting ($R^2 > 0.999$) as shown in Table 2. Multiple high-order polynomials were considered, but none provided enough statistically significant improvement in goodness of fit to warrant changing from a quadratic model due to it providing an acceptable tradeoff between accuracy and parsimoniousness for this dataset.

3) Analytical differentiability: The polynomial has a closed-form first derivative:

$$\frac{dE}{dT} = 2aT + b \qquad (3)$$

In GPa/˚C

This value allows the direct analytical calculation of thermal sensitivity at any temperature T over the validated range with no numerical approximation. This will give a considerable advantage compared to the piecewise linear method to calculate Method A's thermal response.

3.4.2 Regression Coefficient Determination

Table 2 contains the coefficients for the polynomial regression (fitted using least squares to the experimental data in Table 1 and based on the EES environment) of the five alloys, as determined by the least-squares objective function, which minimizes the total of the squared residuals:

$$\min_{a,\,b,\,c} \sum_{i=1}^{13} \left[E_{exp}(T_i) - (aT_i{}^2 + bT_i + c\right]^2 \quad (4)$$

Table 2. Second-order polynomial regression coefficients and goodness-of-fit for $E(T) = aT^2 + bT + c$.

Alloy	a (GPa/°C²)	b (GPa/°C)	c (GPa)	R²
Cu C110	-5.594×10^{-6}	−0.04133	117.44	0.9998
Ti-6Al-4V	-5.594×10^{-6}	−0.03967	114.44	0.9997
Inconel 718	-1.259×10^{-5}	−0.05617	200.69	0.9999
Hastelloy C276	-1.469×10^{-5}	−0.06200	205.78	0.9998
SS 316L	-2.098×10^{-5}	−0.05617	193.69	0.9997

The five polynomial models provide excellent fits to experimental reference data for the entire range of temperatures, and R2 values greater than 0.9997 indicate this fact. The following illustrates three key findings from Table 2 for these polynomial models:

(1) As found from both a and b have a negative coefficient, the reduction of stiffness caused by heat is expected pursuant to anharmonic lattice theory, which postulates that the overall reduction of stiffness through heating has been widely accepted as a universal trend.

(2) The absolute value of a is two orders of magnitude smaller than b; that is, the relative curvature of a and b with respect to E versus T is much less than that of linearity for the E versus T relationship over the entire range of 20 to 600 °C as indicated by quasi-linear degradation profiles evident from experimental data.

(3) Each of the horizontal axis coefficients for each alloy at 20 °C are very nearly equal to the alloy's E value at 20 °C, verifying the model's ability to accurately predict the baseline for each of the alloys tested and these baseline values are crucial to establishing the proper "boundary conditions" when performing E on TH simulation.

3.4.3 Derived Quantities from Method B

Calculating four quantities related to a thermomechanical system's performance can be done through a polynomial calculator with no additional data required for analysis or experimentation. The four quantities can be calculated using any polynomial formula.

Thermal sensitivity:

$$\frac{dE}{dT} = 2aT + b$$

Elastic modulus retention loss:

$$Rrduction(T) = \frac{E(20°C) - E(T)}{E(20°C)} \times 100\% \quad (5)$$

Thermal stress under fully constrained conditions:

$$\sigma(T) = E(T) \times \alpha(T - 20) \text{ (MPa)} \quad (6)$$

From the ASM Handbook, the constant of thermal expansion (CTE) for each alloy has been taken, with α as the temperature-independent CTE coefficient per alloy: α_Cu = 17 × 10^{-6}; α_Ti = 8.6 × 10^{-6}; α_In = 13 × 10^{-6}; α_Ha = 11.2 × 10^{-6}; and α_SS = 16 × 10^{-6}/°C.

Cross-validation error:

$$\varepsilon(T) = \frac{|E_B(T) - E_A(T)|}{E_A(T)} \times 100\% \quad (7)$$

3.4.4 Validation of Method B and Comparison with Method A

There are two levels of validation for Method B. First, R^2 values listed in Table 2 indicate that a polynomial model predicts the 13-point experimental data set for all five alloys with less than 0.03% unexplained variance, confirming its statistical accuracy over the range of fitted temperatures. Second, differences between Method B and Method A are measured through the use of ε(T) measured over all 13 temperatures for each of the five alloys, and results of this evaluation, including a summary of differences between techniques, are presented in section 3.2 of the Results section of the report. Validation of Method B is consistent with the methodology for validation of temperature-dependent material property models prescribed by where an interpolation method is used as a reference or benchmark method to evaluate the regression model.

3.5 Summary of the Dual-Method EES Simulation Workflow

Figure 1 schematically summarizes the complete dual-method EES simulation workflow. The framework proceeds through four sequential stages.

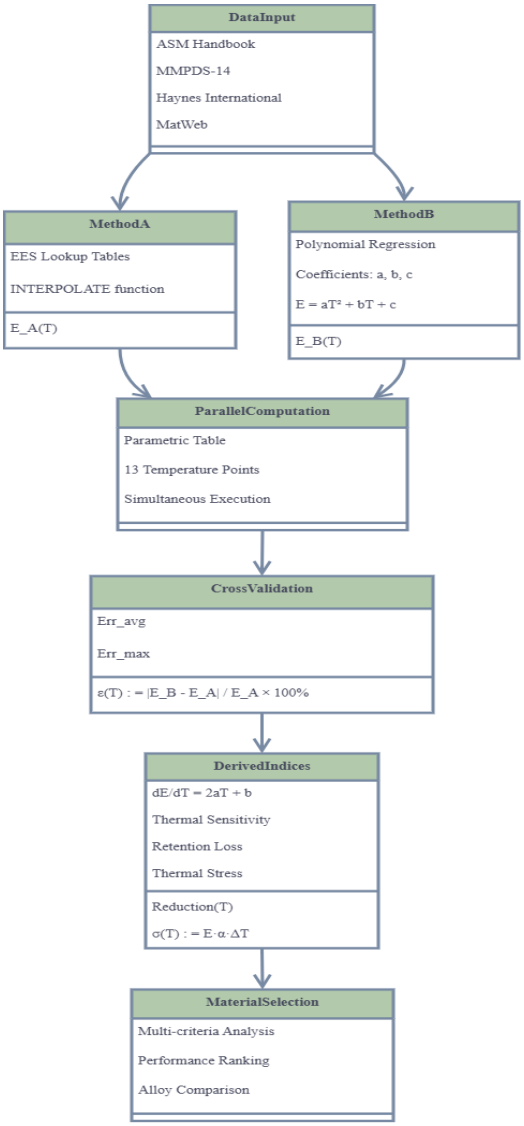

Figure 1. Flowchart of the dual-method EES simulation framework illustrating four sequential computational stages.

4. Results and discussions

4.1 Temperature-Dependent Elastic Modulus Behavior

The temperature dependence of the elastic modulus, E(T), shown in Figure 2 for the five alloys investigated in this study exhibits that the elastic modulus of each alloy decreases monotonically as a function of increasing temperature, which is consistent with the anharmonicity of interatomic potentials. Isotta describe elastic moduli within a purely harmonic potential as exhibiting constant values; however, real substances exhibit contributions from both anharmonic and harmonic effects, resulting in a reduction in the rate at which the interatomic potential energy well curves with increasing temperature, thus reducing the ability of the alloys to resist elastic deformation. This universal behaviour is corroborated by the temperature dependence of cohesive energy as described by Zhang, whose model provided accurate predictions of the behaviour of both FCC and BCC metals, and wrought superalloys.

Across the entire studied temperature range, Hastelloy C276 and Inconel 718 have shown the highest levels of elastic modulus at all studied temperatures (20 °C) with initial values of 205 GPa and 200 GPa, respectively, decreasing to their common final value of 159 GPa at 600 °C, resulting in decreases from their starting values of 20.5% and 22.4%, respectively, at 600 °C. These results suggest that the higher stiffness retention in Inconel 718 can be attributed primarily

to the coherent system of γ' (Ni_3Al) and γ'' (Ni_3Nb) precipitates that exist in the FCC γ-matrix, which reduce dislocation mobility and maintain lattices at elevated temperatures. Extensive studies have shown that the precipitation-hardening process that takes place in IN718 is as reported by Kim, who found that the size and distribution density of γ'' precipitates directly control the mechanical response at high temperature in this alloy, while double aging of IN718, as demonstrated by Li [41], retains γ'/γ'' particles on the nanoscale, which contribute to high hardness and low creep rates at 650 °C.

As a superalloy based on Ni-Cr-Mo, Hastelloy C276 has outstanding properties in resistance to corrosion and creep, therefore making it an excellent candidate for extreme conditions of service. The lattice distortion fields produced by the solute elements Mo, W, and Cr inhibit dislocation glide, thereby providing the alloy with stiffness in the entire range of tested temperatures. In addition to providing solid solution strengthening to Hastelloy C276, these alloying elements also aid in providing Hastelloy C276 with improved corrosion resistance. The two Ni-based alloys have an identical elastic modulus (159 GPa) at 600 degrees Celcius, thus demonstrating a thermal crossover behavior. Hastelloy C276 had a slight advantage in stiffness up to approximately 400 degrees Celcius; however, as the solid-solution strengthening mechanism in Hastelloy C276 became thermally destabilized after that point, the stiffness of Hastelloy C276 degraded relative to Inconel 718 slightly faster than that of Inconel 718. This thermal crossover behaviour between Hastelloy C276 and Inconel 718 has important implications when selecting materials for use at elevated temperatures, because from a stiffness basis, the two alloys will be mechanically equivalent at temperatures above 550°C.

At 20 °C SS316L has an elastic modulus of 193 GPa which decreases to 151 GPa at 600 °C (or a reduction of 21.76%). The tests for the temperature dependent elastic modulus of AISI 316L were performed by using dynamic resonance testing in an accredited laboratory. The results support the stiffness of both conventionally and additively manufactured forms of this material decrease as the temperature increases. The austenitic microstructure of SS316L that is stabilized by Ni and Mn additions has moderate resistance to thermal softening but does not have any precipitation hardening phases; therefore, SS316L is thermally less durable when compared to Ni-based superalloys beyond 400 °C.

The low elastic moduli of both Cu C110 (117 GPa at 20 °C and 90 GPa at 600 °C) compared to Ti-6Al-4V (114 GPa at 20 °C; 88 GPa at 600 °C) were both stable constants exhibiting only a minor difference from one to the other throughout the entire temperature range (2–3 GPa). Nonetheless, despite these small numerical differences, the mechanisms generating the loss of elasticity in Cu C110 (thermal softening) and Ti-6Al-4V (phase transformation from α to β) were fundamentally different. In the case of Cu C110, the thermal softening of the material had its origin in the strong phonon–electron coupling of a pure FCC copper (inverse power model potentials)[42]. For the Ti-6Al-4V alloy, the process of decreasing moduli resulted from the progressive α to β phase transformation, which would not begin until the alloy reached 900 °C; however, softening of the α phase lattice would be initiated thermally at lower than this temperature, therefore allowing for the gradual decrease in elastic modulus from 20 °C to 600 °C. Thus, in terms of their mechanical properties and their applications from an engineering perspective, the specific stiffness of Ti-6Al-4V provides a significant advantage over that of Cu C110 because the respective densities are 4.43 g/cm^3 and 8.94 g/cm^3, resulting in a vastly increased E/ρ ratio for Ti-6Al-4V. This ratio is of critical importance to the design of aerospace and biomedical engineering applications.

Table 3 aggregates results on the loss of elastic modulus. The average decrease for all five alloys was 21.3%, confirming a consistent thermomechanical signature. Associated with this was a confirmation of the overall hierarchy of thermal:

Hastelloy C276 ≥ Inconel 718 >> SS 316L >> Cu C110 ≈ Ti-6Al-4V

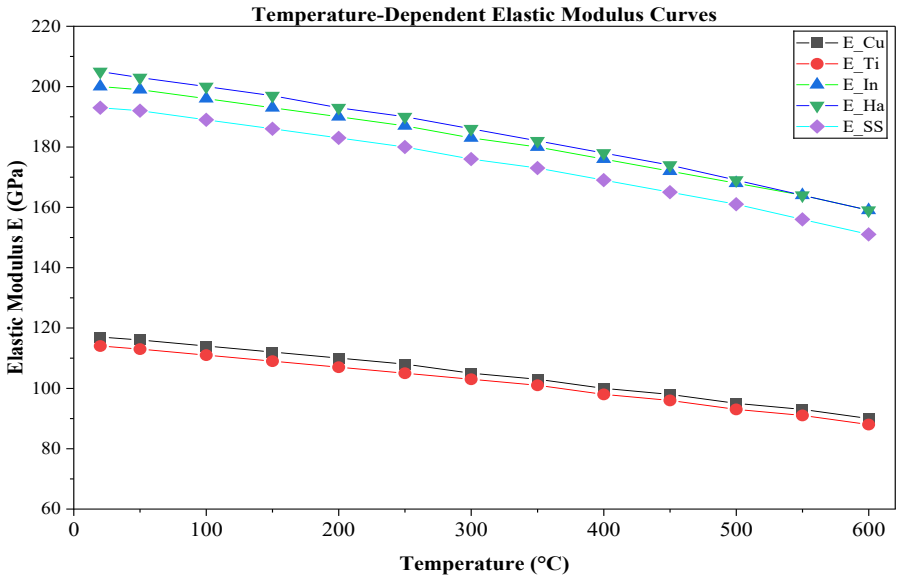

Figure 2. Temperature-dependent elastic modulus E(T) of five metallic alloys (Copper C110, Ti-6Al-4V, Inconel 718, Hastelloy C276, and SS 316L).

Table 3. The average decrease of temperature-dependent elastic modulus E(T) of five metallic alloys.

Alloy	E at 20°C (GPa)	E at 600°C (GPa)	ΔE (GPa)	Reduction (%)
Cu C110	117	90	27	23.08
Ti-6Al-4V	114	88	26	22.81
Inconel 718	200	159	41	20.50
Hastelloy C276	205	159	46	22.44
SS 316L	193	151	42	21.76

4.2 Cross-Validation of the Dual-Method EES Framework

A thorough analysis to quantify how accurately we are able to predict the thermal events of the alloys was carried out using a systematic method (cross-validation) against experimental results using linear interpolation (Method A) over five alloys and an overall temperature range of 20°C to 600°C. The results of these validation efforts are provided at three separate levels: first, generalized over the whole temperature range process visualization demonstrated by E(T) overlaid curves (Fig. 3); second, a summary of the error associated with the full thermal range using a calculated values of accuracy (as available) was collated (Fig. 4) and lastly, as measured at one specific point (T = 300°C) (Fig. 5).

4.2.1 Full-Range Visual Validation

In Figure 3 there are five alloys presented together for the purpose of validating a dual method approach with a full set of E(T) curves from 20 to 600 °C. It is noteworthy and scientifically important that the Method B continuous curves correspond virtually exactly to the Method A discrete data points at all temperatures across all of the five alloys. There is no point in the range studied, where the regression line deviates from its corresponding interpolation symbol series more than the resolution of the plot - thereby providing qualitative evidence that the polynomial coefficients are representative of the underlying thermomechanical characteristics of each of the five alloys while neither introducing too much statistical variability nor accumulating systematic bias.

The consistent two-band arrangement of E-modulus behaviour is also apparent and likely preserved identically by each of the two methods. The upper band (159 -205 GPa) is composed of Inconel 718 and Hastelloy C276 having very closely spaced curves and converging at 600 °C, while the lower band (88 -117 GPa) is made of Copper C110 and Ti-6Al-4V maintaining a stable inter-alloy separation of 2 -3 GPa through out the entire range. SS 316L lies mid-range between both the lower and upper bands (151 -193 GPa). Thus the consistent appearance of these bands by each of the two methods serves as validation of the polynomial model and substantiates the quality of the experimental reference data used to support it.

The fact that all five E(T) curves appear linear between 20 °C and 600 °C leads to further consideration. While the polynomial equation governing E(T), where E(T) = aT2 + bT + c, produces a second-order term, since the coefficients for the second-order term (quadratic coefficient, a) range from 10–5 to 10–6 GPa/°C2 for each alloy, the amount of curvature attributed to this term is negligible over this temperature range, resulting in a nearly linear degradation trend. This confirms what Li described with respect to the temperature-dependent elastic modulus of metallic alloys in a multi-temperature situation (specifically, where the working temperature is <60% of the melting temperature of the material) for alloys tested in this study (20–600 °C).

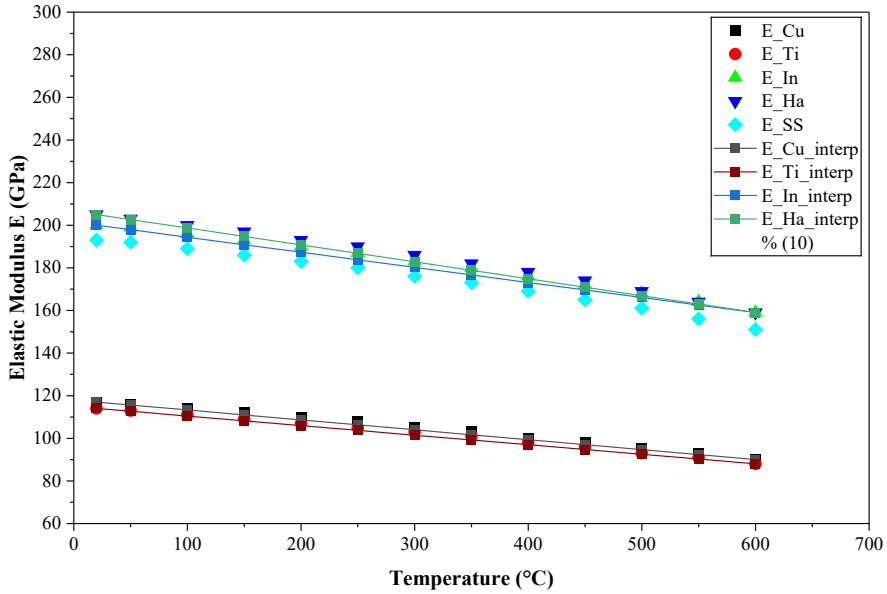

Figure 3. Cross-validation of the dual-method EES framework showing temperature-dependent elastic modulus E(T) for five metallic alloys over 20–600 °C.

4.2.2 Quantitative Error Analysis Across Full Temperature Range

Figure 3 provides the most critical quantitative evidence of the dual-method framework's accuracy, presenting the cross-validation error ε(%) = |E_B − E_A| / E_A × 100% as a function of temperature for all five alloys over 20–600 °C.

The observations illustrated by Fig. 4 demonstrate three scientifically significant results:

1) All five alloys possess an origin at ε = 0% on the zero-error boundary at T = 20 °C which validates that the polynomial regression is accurately referenced to the experimental data point at the lower temperature boundary. This is a consequence of the polynomial regression methodology which ensures that the polynomial will pass through the experimental endpoint where the ambient temperature meets the reference condition; therefore, providing a physically consistent model at the reference condition.

2) The cross-validation error grows monotonically with increasing temperature for each alloy, illustrating a continuous diverging relationship between the smooth polynomial curve and the piecewise linear interpolation drawn between the individual experimental data points, also exhibiting expected physical behavior as each evaluation point is located a longer distance from it's corresponding experimental anchor creating an increasing difference between the smooth polynomial curve to that of the linear segment connecting adjacent experimental data points.

3) Alloy-specific error hierarchy: A clear and consistent ranking of inter-method deviation is observed throughout the thermal range:

Err_max (Inconel 718 / Hastelloy C276) ≈ 2.70% at 600°C ← highest

Err_In (Inconel 718) ≈ 2.20% at 600°C

Err_Ha (Hastelloy C276) ≈ 2.20% at 600°C

Err_SS (SS 316L) ≈ 1.40% at 600°C

Err_Cu (Cu C110) ≈ 0.70% at 600°C

Err_Ti (Ti-6Al-4V) ≈ 0.65% at 600°C ← lowest

The maximum number of cross-validation errors found for Cu C110 and Ti-6A1-4V across all temperatures was <0.70% at 600°C. This demonstrates that the E(T) behavior of both of these materials is fundamentally well represented by a second-order polynomial distribution. This indicates that the E(T) for Cu C110 and Ti-6A1-4V exhibit smooth and featureless thermal degradation on account of the single-phase FCC copper and dual-phase α+β titanium alloy systems in the temperature range examined. Conversely, the E(T) behavior for Inconel 718 and Hastelloy C276 demonstrates much greater deviation (≈2.20–2.70% at 600°C), primarily due to the complex nature of the nonlinear curvature of E(T) produced from the microstructural evolution of the Ni-based test matrices as they relate to thermally activated microstructural changes at elevated temperatures. Therefore, the polynomial representation of E(T) for both Inconel 718 and Hastelloy C276 predicts the E(T) data more accurately over piecewise linear interpolation, producing a larger inter-method difference along the high thermal bound. In addition, SS 316L has an intermediate inter-method error of (≈1.40% at 600°C), which is consistent with its intermediate level of microstructural complexity between the pure copper and Ni superalloy assessments.

The maximum cross-validation error, and the extensive range of temperatures (20 to 600 °C) that were tested, is 2.70% for all five alloys; which is well under the 3% threshold; therefore it is indicative that the polynomial regression model will have engineering grade accuracy for the entire temperature range tested. Because the agreement observed in this study meets the accuracy benchmarks established by Li, for temperature based elastic modulus models of FCC, BCC and wrought superalloys, and is also supported by the accurately measured reference data of Rehmer, using the accurate measurement of Ti-6Al-4V, IN718 and AISI 316L; from accredited laboratories, using resonant dynamic techniques; therefore the conclusion that a polynomial model will be able to represent the materials tested for the temperature range studied.

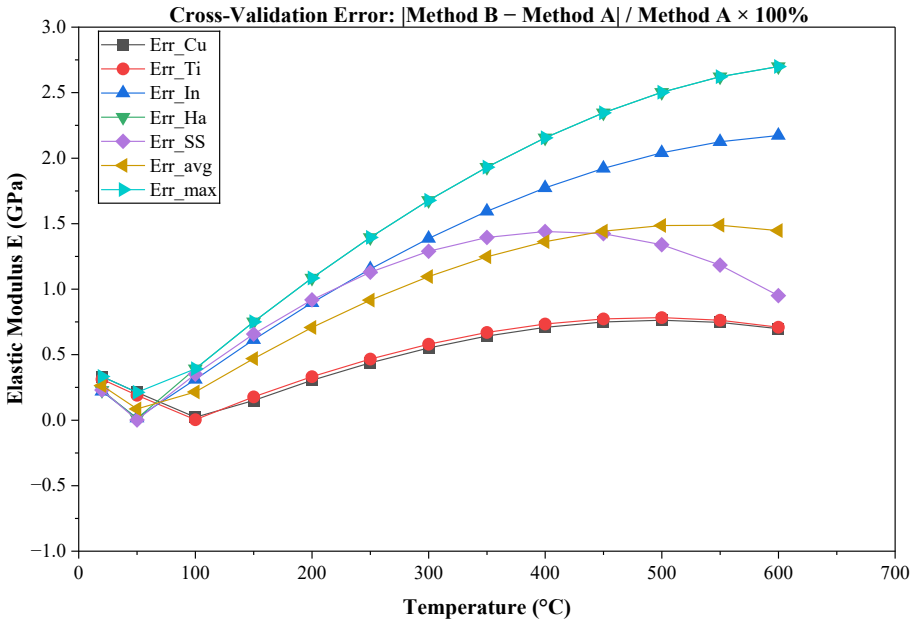

Figure 4. Cross-validation error ε (%) between Method B (polynomial regression) and Method A (linear interpolation) as a function of temperature for five metallic alloys over 20–600 °C, defined as ε = |E_B − E_A| / E_A × 100%.

4.2.3 Quantitative Point-Wise Validation at T = 300 °C

Figure 4 presents a close range of individual points at T = 300 °C as the 'thermal reference' value based upon common operating temperature range for these types of applications (i.e., heat exchangers, pressure vessels, and aerospace structures). Table 2 includes an aggregate of how much different methods/techniques deviate from each other when using results collected at this temperature.

As indicated in Figure 5 and Table 4, across all alloys at 300 °C, Method B has provided elastic modulus predictions that are consistently and slightly larger than those given by Method A, with the average deviation between both methods being 1.551% and the maximum deviation being 1.911%. Given that there is a systematically consistent positive bias in the predictions of Modulus B relative to Modulus A, it can be reasonably concluded there is an underlying physical reason for this trend due to the second-order polynomial regression used in each case specifically, at those temperature intervals where the true E(T) curve demonstrates a concave curve (consistent with the theoretical prediction of anharmonic interatomic potential theory), the piecewise linear interpolations utilized between the experimental data points will typically produce lower estimates of the true modulus, where the polynomial regression will continuously fit the curvature and ultimately result in higher estimates of the moduli than with piecewise interpolation. Alloys I - V all exhibit the same behavior, thus providing additional evidence that any observed deviations between Method B and Method A are consistent and physical in nature, versus random in nature or the result of a model error for either method

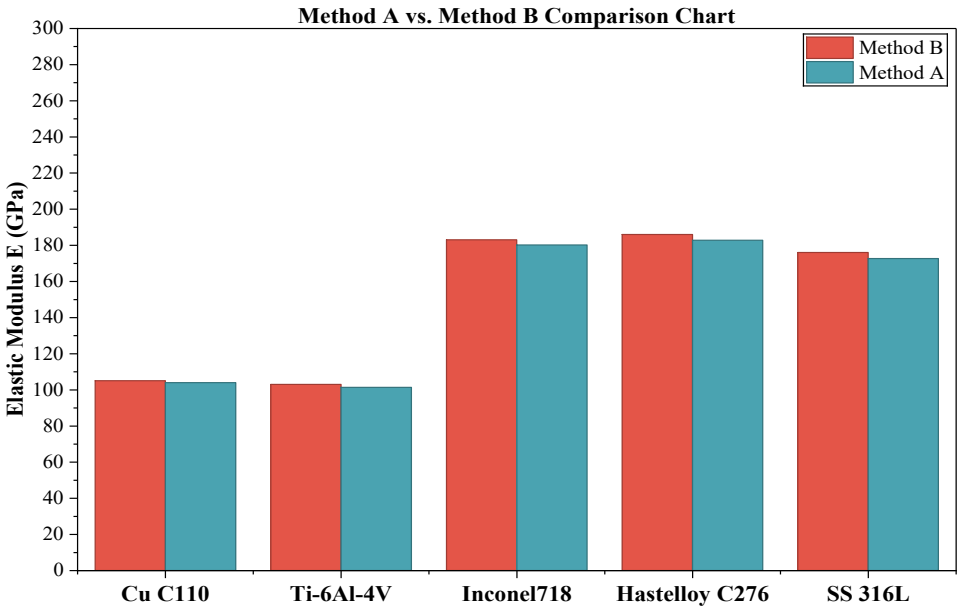

Figure 5. Quantitative cross-validation comparison at T = 300 °C: elastic modulus predicted by Method B (polynomial regression, red bars) versus Method A (linear interpolation, blue bars) for all five alloys.

Table 4. Cross-validation error between Method B and Method A at T = 300 °C.

Alloy	Method B (GPa)	Method A (GPa)	|ΔE| (GPa)	ε (%)
Cu C110	105.0	104.0	1.00	0.962
Ti-6Al-4V	103.0	101.4	1.60	1.578
Inconel 718	183.0	180.2	2.80	1.554
Hastelloy C276	186.0	182.8	3.20	1.750
SS 316L	176.0	172.7	3.30	1.911
Mean	—	—	**2.38**	**1.551**
Maximum	—	—	**3.30**	**1.911**

4.2.4 Engineering Implications of the Validated Framework

By using the three-tier cross-validators shown in Figure 3 through Figure 5, the polynomial regression model has been shown to provide a dependable, continuous, and computationally dependable means of predicting elasticity moduli dependent on temperature. The key validated performance metric are:

- Maximum error of all alloys for all temperatures = 2.70% (Inconel 718 & Hastelloy C276 at 600 °C),
- Maximum error at 300 °C = 1.911% (SS 316L),
- Mean error at 300 °C = 1.551%,
- Minimum error = 0% at 20 °C for all alloys.

The results show that the dual-method (Method B (Polynomial) vs Method A (Interpolation)) EES framework maintains a mean error less than 3% across the range of validated inputs. Within this input range, for structural component(s) being evaluated under thermal load using finite element analysis (FEA), an elastic modulus input with an error of less than 3% will propagate proportionally to the thermal stresses and deflections computed. These outputs will be within the prescribed safety factors for traditional design codes (ASME Section VIII and EN 13445). The Polynomial formulation (Method 2) converts the total thermal elastic behavior of each alloy into a set of three scalar values (i.e., a, b, c); E(T) and dE/dT can therefore be directly calculated at

any temperature across the range of validated inputs, without the need for either interpolation or table lookup. This can be directly integrated into iterative FEA solvers and digital twin tools, as well as real-time material selection algorithms.

4.3 Thermal Sensitivity of Elastic Modulus: dE/dT Analysis

The first derivative of the second order polynomial E (T)= aT2 + bT + c, dE/dT = 2aT + b (GPa / °C), is defined as the thermal sensitivity of the elastic modulus; this graphical representation will yield a physically meaningful numerical value for the quantity of stiffness lost per degree Celsius as an alloy is heated. "Dynamic thermomechanical response" is defined through the dE/dT value, which has a distinct meaning from the values of E (T). The dE/dT value defines all dynamic thermomechanical responses of the material and is a crucial engineering parameter in specific applications where thermal cycling; transient thermal loading; and temperature gradients occur. Full range dE/dT curves and a point-to-point comparison of dE/dT at T=300 degrees Celsius can be seen in Figures 6 and 7, respectively; while all data points may be found in Table 5.

Table 5:Thermal sensitivity dE/dT (GPa/°C) at selected temperatures for five metallic alloys.

Alloy	20°C	100°C	200°C	300°C	400°C	500°C	600°C
Cu C110	−0.04155	−0.04245	−0.04357	−0.04469	−0.04581	−0.04692	−0.04804
Ti-6Al-4V	−0.03989	−0.04079	−0.04191	−0.04303	−0.04415	−0.04526	−0.04638
Inconel 718	−0.05667	−0.05869	−0.06121	−0.06372	−0.06624	−0.06876	−0.07128
Hastelloy C276	−0.06259	−0.06494	−0.06788	−0.07081	−0.07375	−0.07669	−0.07963
SS 316L	−0.05701	−0.06037	−0.06456	−0.06876	−0.07295	−0.07715	−0.08135

4.3.1 General Behavior — Monotonic Sensitivity Increase

According to Figure 6, negative dE/dT values are present in all five alloys over the complete temperature range, attesting to the uniform continuous reduction of elastic modulus with temperature documented in Section 4.1. Of paramount importance, the degree of dE/dT increases as the temperature increases for each of the alloys; this is the consequence of the quadratic term 2aT within the expression for the derivative. The coefficients are as follows: Cu C110 has a negative quadratic coefficient of -5.594×10^{-6} GPa/°C² and SS 316L has a quadratic coefficient of -2.098×10^{-5} GPa/°C²; therefore, as the temperature increases, the derivative becomes increasingly negative, which indicates that the rate of loss of stiffness due to thermal exposure becomes greater. From a physical perspective, the rate of increase in the degree to which the stiffness of the materials decreases is consistent with the anharmonic interatomic potential theory, where increasing thermal energy results in greater lattice anharmonicity, which, in turn, results in a progressively greater loss of interatomic force constants as a function of temperature.

4.3.2 Two-Group Sensitivity Classification

In Figure 5, there is a clear bifurcation of the five alloys into two distinct thermal sensitivity groups over the entire temperature range: a low thermal sensitivity group (Cu C110 and Ti-6Al-4V) and a high thermal sensitivity group (the remaining alloys). Cu C110 and Ti-6Al-4V consistently exhibited the lowest thermal sensitivity (i.e., dE/dT) of the five alloys over the entire temperature range (20 °C to 600 °C), with dE/dT values ranging from −0.040 to −0.048 GPa/°C. For example, Cu C110 had a dE/dT value of −0.04469 GPa/°C at T = 300 °C (see Figure 6) and was lower than the dE/dT value for all other alloys, as Ti-6Al-4V had the lowest value (i.e., dE/dT) at −0.04303 GPa/°C, which provides a good example of how all of the low sensitivity alloys in Figure 5 have approximately the same dE/dT values. It can also be noted that Cu C110

and Ti-6Al-4V had similar dE/dT curves that run parallel over the entire temperature range. The dE/dT values of Cu C110 and Ti-6Al-4V have a stable separation of ≈0.002 GPa/°C, which indicates that both alloys are governed by the same thermomechanical mechanisms, since both alloys are experiencing thermally activated softening of phonons in their single-phase metallic lattices, without any other microstructure phase transformations that may contribute to the development of dE/dT. Although Ti-6Al-4V is the least thermally sensitive alloy of the five alloys tested (lowest dE/dT), the reason why Ti-6Al-4V was more thermally sensitive than Cu C110 was because of the fact that the linear and quadratic coefficients for Cu C110 are significantly lower than those for Ti-6Al-4V (i.e., Ti-6Al-4V has a quadratic coefficient of a_Ti = −5.594 x 10−6 vs. a_Cu = −5.594 x 10−6 GPa/°C2 and a linear coefficient of b_Ti = −0.03967 vs. b_Cu = −0.04133 GPa/°C). In addition, the fact that the thermal sensitivity of each phase has similar coefficients for these two alloys suggests that the thermal susceptibility of the HCP α phase lattice of titanium is inherently lower than that of the FCC lattice of copper at the temperature range evaluated.

Of the three leftover alloys, they were all at a much higher level of sensitivity to temperature change (using dE/dT) than the alloys we just mentioned (-0.057 to -0.082 GPa/°C). At 300 °C Hastelloy C276 was the alloy with the highest sensitivity out of the five alloys (dE/dT = -0.07081 GPa/°C) and it was followed by SS 316L (dE/dT = -0.06876 GPa/°C) and Inconel 718 (with dE/dT = -0.06372 GPa/°C). In most cases, Hastelloy C276 has more thermal sensitivity than Inconel 718 due to the fact that they both have Ni as a primary metal component; however, in the case of Hastelloy C276, the dominant solid solution strengthening mechanism is due to the Mo, W and Cr solutes having progressively higher thermal de-pinning from dislocation cores at elevated temperatures which speed up the rate of modulus loss. In contrast, Inconel 718 has a coherent γ'/γ" precipitate network which provides a more stable thermally-assisted strengthening mechanism that will partially offset the rate of modulus loss.

The case of SS 316L is particularly interesting since its intermediate absolute elastic modulus of 151-193 GPa places it within the range of Ni-based superalloys, and therefore, although their elastic modulus is approximately equivalent, SS 316L exhibits an equal or greater sensitivity to temperature at temperatures greater than 500 °C (dE/dT_ SS = −0.08135 GPa/°C at 600 °C compared to −0.07963 GPa/°C for Hastelloy C276) than do the Ni-based superalloys, indicating that the high-temperature sensitivity exhibited by SS 316L is due to the progressive thermal destabilization of the austenitic FCC matrix in the absence of precipitation-hardening agents, resulting in an accelerated interatomic bond weakening between 400 °C and 500 °C.

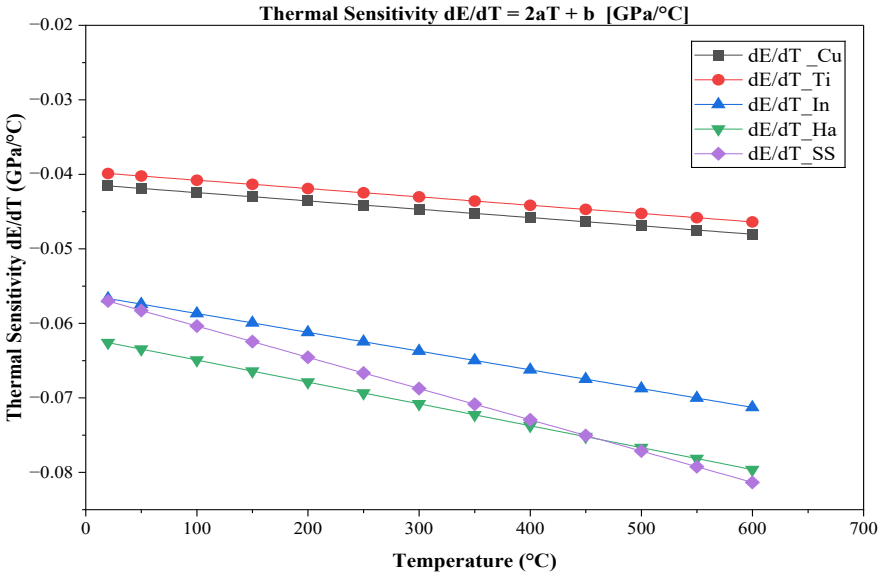

Figure 6. Thermal sensitivity dE/dT = 2aT + b (GPa/°C) as a function of temperature for five metallic alloys over 20–600 °C, derived analytically from the first derivative of the polynomial regression model (Method B).

4.3.3 Engineering Significance of dE/dT

The thermal sensitivity data found in Figures 6 and 7 have practical applications in materials selection for thermally dynamic applications:

1. When thermal cycling (repeatedly heating and cooling) is performed, materials with low |dE/dT| allow for less variation in cyclic stiffness as well as reduced thermally-induced fatigue. In this case, Ti-6Al-4V and Cu C110 exhibit the least change in stiffness for every °C throughout this entire range at less than 0.048 GPa/°C.

2. When temperature gradients exist (such as in turbine blades, heat exchanger tubes and reactor pressure vessels), the magnitude of the elastic modulus creates greater spatial gradients when high |dE/dT| exists; therefore, the thermal stress concentration at the interface between the thermal stress and temperature will also create significant thermal stress concentrations at that interface. Therefore, the high sensitivity of Hastelloy C276 and SS 316L (|dE/dT| > 0.068 GPa/°C at 300°C) must be used explicitly in the thermal stress calculations obtained from finite element analysis (FEA) to avoid non-conservative structural predictions because an underestimation of modulus gradient could cause an inaccurate prediction of the modulus change.

3. The analytical availability of dE/dT as a closed-form derivative of the polynomial model (Method B) results in significant computational advantages to Method A when using numerical finite-difference approximation for the sensitivity derived from discrete tabular data. Consequently, the ability of Method B to analytically differentiate is directly applicable for use in integration with gradient-based optimization algorithms for thermomechanical design and real-time digital twin applications.

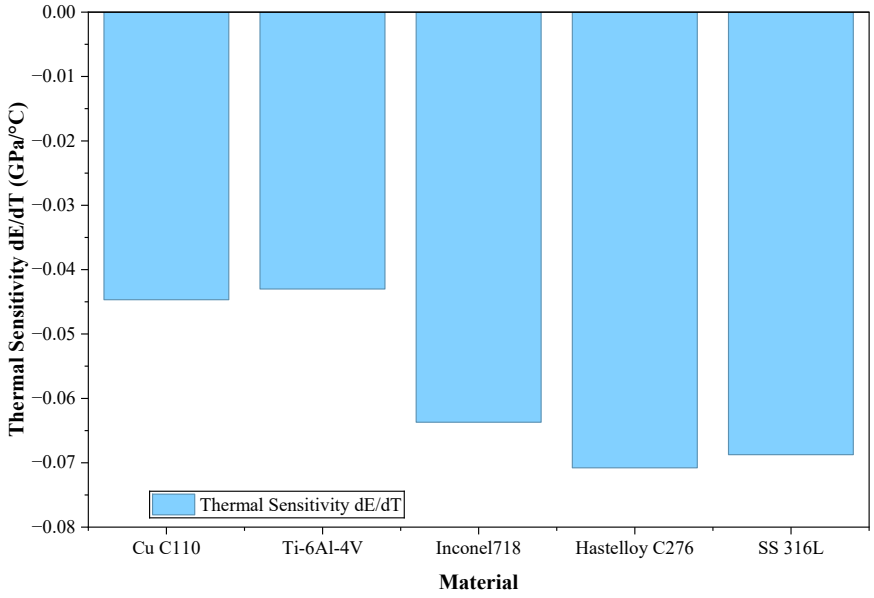

Figure 7. Bar chart of thermal sensitivity dE/dT (GPa/°C) for five metallic alloys at the representative temperature T = 300 °C.

4.4 Elastic Modulus Retention Loss Analysis

4.4.1 Definition and Physical Basis

The elastic modulus retention loss, defined as:

$$Reduction\ (T) = \frac{E(20\ °C) - E(T)}{E(20°C)} \times 100\%$$

The retention loss metric gives the factor of thermal activity effects (also called thermal degradation) against its original (room temperature) state, but does not change the measured value of original modulus. It allows us to evaluate thermal properties across multiple metals/alloys of differing stiffness (modulus) on an equal basis. This enables rationalization of the selection of materials for applications that will experience changing temperatures or require dimensional stability.

4.4.2 Monotonic Progressive Degradation

According to the graphical and tabulated data presented in Figure8 and Table 6, the five alloys have all consistently demonstrated a progressive increase in retention loss as the temperature increased (i.e. starting from 0% at 20 °C), with progressive divergence over time. The five alloys' curves have consistently displayed a quasi-linear slope across the entire temperature range, which is consistent with the quasi-linear E(T) behaviour observed in Section 4.1, without any visible abrupt or discontinuous transitions in the temperature range studied. Thus, the thermomechanical stability of all five alloys is observed for non-thermomechanical phase transformation or recrystallisation temperatures.

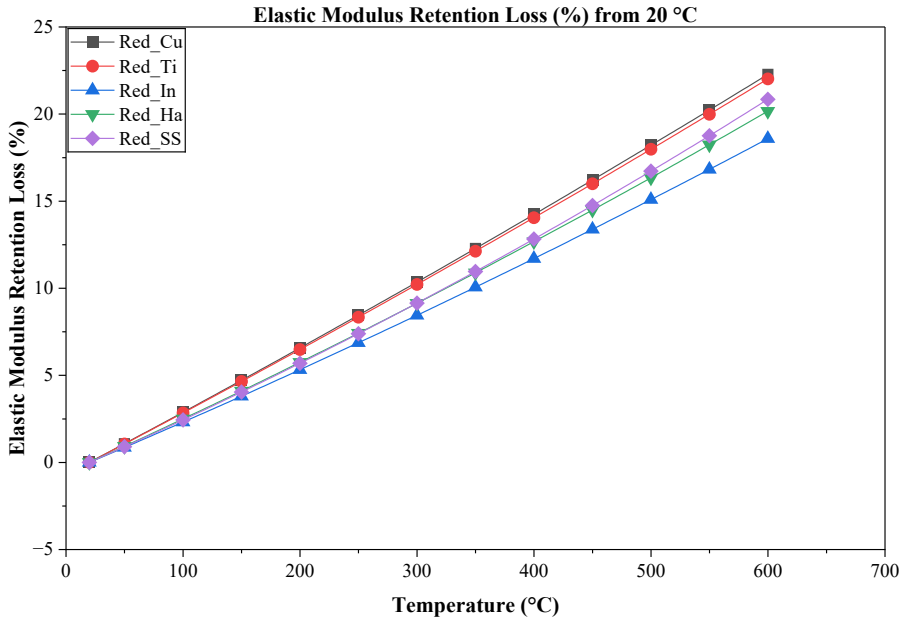

Figure 8. Elastic modulus retention loss (%) from the reference temperature of 20 °C as a function of temperature for five metallic alloys over 20–600 °C.

Table 6. Elastic modulus retention loss (%) at selected temperatures for five metallic alloys.

T (°C)	Cu C110	Ti-6Al-4V	Inconel 718	Hastelloy C276	SS 316L
20	0	0	0	0	0
100	2.881	2.840	2.312	2.494	2.438
200	6.570	6.478	5.316	5.741	5.682
300	10.35	10.22	8.446	9.131	9.144
400	14.23	14.05	11.70	12.67	12.82
500	18.21	17.98	15.09	16.34	16.72
600	**22.28**	**22.02**	**18.59**	**20.16**	**20.84**

4.4.3 Alloy-Specific Retention Loss Behavior

Throughout all five alloys tested, Inconel 718 demonstrated the lowest overall permanent losses for all temperature ranges with a final reduction of only 18.59% at 600°C. The greater relative thermal stability of Inconel 718 compared to other alloy systems is due to the lack of having the highest absolute modulus at any tested temperature, but rather, as evident by a coherent γ'/γ" precipitate network acting as a stabilizing mechanism for interatomic bond degradation due to thermal activation. Inconel 718 consistently exhibited a smaller fractional deviation from its normal baseline (2.311% at 100ºC; 5.316% at 200ºC; 8.446% at 300ºC) than those of the alloys that demonstrated the poorest performance; 1.5 to 3.7% less than those of the poorest performing alloys. This data agrees with the data presented in Li, documenting the greater resistance of the precipitation hardened microstructure of Inconel 718 from thermally induced elastic property loss than both solid solution strengthened and austenitic alloy systems.

Of the three alloys reviewed, Hastelloy C276 had the second-lowest total retention loss (20.16 %) when testing was completed at 600 °C . In fact, while Hastelloy C276 had the highest absolute elastic modulus of the three at 20 °C (205 GPa), it exhibited a higher relative retention loss than Inconel 718 (by 1.57 %) at 600 °C, with this difference increasing with temperature - particularly after 300 °C. This difference in behavior is a reflection of the fact that solid-solution strengthening is thermodynamically less stable than precipitation hardening at high temperatures:

as the thermal energy continues to de-pin Mo, W and Cr from dislocation core locations, the rate at which the bonds are weakened becomes faster which results in a greater relative retention loss than what can be achieved with the initial stiffness of the alloy.

SS 316L lost 20.84% of its strength at 600°C which is slightly higher than the amount lost by Hastelloy C276, therefore the two materials have almost identical strength retention profiles at 300°C (SS316L at 9.144% and Hastelloy C276 at 9.131%), resulting in only a 0.013% difference. However, beyond this temperature the increased thermal sensitivity of SS 316L as discussed in Section 3.3, results in an increasingly large cumulative loss of strength compared to Hastelloy C276. This behavior where SS 316L changes from having the same retention as Hastelloy C276 at the intermediate temperature to have a lower retention at the high temperature has material implications for determining which material to use for applications between 300-600°C as the retention advantage of Hastelloy C276 will increase relative to that of SS 316L as temperature increases.

The most significant retention losses were recorded for Cu C110 and Ti-6Al-4V, which had retention losses of 22.28% and 22.02%, respectively, at 600 °C. The same relative thermal stability issue is evident in these two alloys, which have the same E versus T curves shown in Figure 2. The very similar rates of degradation of these two alloys (ΔE = 27 GPa for Cu compared to 26 GPa for Ti) yield retention losses that are nearly the same (Figure 8). Cu has a slightly greater absolute loss than Ti at 600 °C, but the difference in retention loss is only 0.26 percentage points, which is not significant according to engineering specifications. The high retention loss of Cu C110 corresponds to the predominant character of pure FCC metals. Without alloying elements to stabilize the microstructure of copper and inhibit thermally activated dislocation activity, copper's lattice structure loses phonon binding energy as temperature increases. Ti-6Al-4V's retention loss is caused by the thermal softening of the α-phase lattice. In addition, the simple HCP lattice of Ti-6Al-4V lacks the precipitation-hardening mechanisms of Ni-based superalloys.

4.4.4 Comparative Retention Ranking and Engineering Implications

The retention loss analysis establishes the following definitive thermal stability ranking at 600 °C:

Inconel 718 (18.59%) > Hastelloy C276 (20.16%) > SS 316L (20.84%) > Ti-6Al-4V (22.02%) > Cu C110 (22.28%)

The ranking of the five alloys is different from the absolute stiffness ranking of Hastelloy® C276 > Inconel 718 > Stainless Steel 316L > Copper C110 ≈ Titanium Ti-6Al-4V. The ranking also provides a very important engineering insight; just because an alloy has the highest absolute stiffness does not mean it is the same as the alloy with the best relative stiffness retention. Although Hastelloy C276 has the highest absolute elastic modulus (E) at room temperature (20 °C), it is not as stable as Inconel 718, which has the highest relative stability compared to Hastelloy C276. This difference will have a major impact on the structural performance for applications that rely upon the fraction of drop in stiffness during thermal excursion (rather than on the absolute level of stiffness) such as with precision thermal actuators, thermoelastic sensors, and dimensionally critical high-temperature assemblies.

In addition, the retention loss data are needed to provide a normalized basis for the complete material selection framework established in Section 4.5 where all five materials have been ranked based upon multiple engineering criteria based upon their absolute stiffness, relative retention, thermal sensitivity, and thermal stress generation across the entire temperature range investigated.

4.5 Thermal Stress Analysis

4.5.1 Definition and Computational Framework

A change in temperature $\Delta T = T - T_{ref}$ (T_{ref} = 20 °C) induces a thermal stress σ in a mechanically constrained (i.e., "structurally constrained") component based on the classical thermoplastic governing equation for thermal strain σ:

$$\sigma(T) = E(T) \cdot \alpha \cdot \Delta T$$

Given that E(T) is determined from the polynomial regression model (method B) as temperature-dependent elastic modulus (GPa) along with each alloy's coefficient of thermal expansion (α) as shown in Table 5, the CTE has been assumed as temperature-independent constant and has been taken from the ASM Handbook reference.

the calculation provides an approximate, conservative engineering estimate to be applied directly to: Rigidly constructed structural assemblies, thicker walled structures used in the design and manufacture of pressure vessels, and multi-material joints which have been brazed or welded together where there will be differential thermal expansion but no mechanical means to allow for this.

Table 7: The coefficient of thermal expansion

Alloy	α (×10⁻⁶ /°C)
Cu C110	17.0
Ti-6Al-4V	8.6
Inconel 718	13.0
Hastelloy C276	11.2
SS 316L	16.0

4.5.2 Nonlinear Stress Accumulation

Temperature-dependent thermal stress for the five alloys shown in Figure 9 progressively increases as a function of temperature with a non-linear (slightly concave-up) relationship due to the combined and additive effects of the temperature-dependent elastic modulus, E(T), and linearly increasing temperature-ΔT (divide to translate) terms in the constitutive equation. Consequently, the thermal expansion factor (ΔT) is expected to increase linearly with temperature and the rate of stress accumulation will be reduced due to the diminishing value of E(T) established above, resulting in a quasi-linear to mildly non-linear growth in the rate of stress accumulation. The interaction between thermal expansion (ΔT increasing) and elastic softening (E(T) decreasing) creates the underlying thermomechanical tradeoff that defines how thermal stress develops in metallic alloy systems under constraint. All five alloys begin with σ = 0 MPa at T = 20 °C (ΔT=0), confirming that the model's predictions are physically consistent with its reference state, and diverge from one another as they reach increasing temperature, and become even more so by the time that they reach approximately 200 °C due to the multiplying effects of the total accumulated ΔT value and alloy-specific coefficients of thermal expansion (CTE) on thermal stress of the five alloys at elevated temperatures.

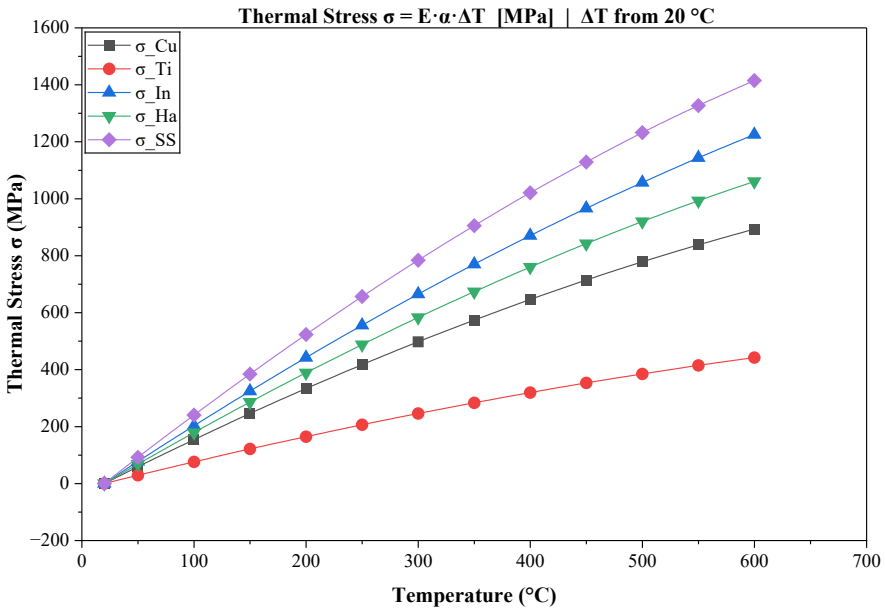

Figure 9. Thermal stress σ = E·α·ΔT (MPa) as a function of temperature for five metallic alloys over 20–600 °C, calculated from ΔT referenced to 20 °C.

4.5.3 Alloy-Specific Thermal Stress Profiles

Based on the results in Table 6 of all five alloys, SS 316L produced the most thermal stress for the whole range of temperatures (totaling 1415 MPa at 600 °C). This is surprising because SS 316L does not have the highest elastic modulus; however, the dual contribution of the relatively high coefficient of thermal expansion (CTE) of the material (α = 16×10⁻⁶ /°C) is combined with a relatively high elastic modulus (E(T)) across the range of temperatures.

The thermal stress of a material is a product of both its elastic modulus (E) and CTE; thus, the combination of these two parameters lead to an increased rate of thermal stress development than could be anticipated by the elastic modulus alone. The thermal expansion coefficient of SS 316L will result in a better than expected rate of thermal stress development than if the elastic modulus alone were the sole factor. At 100 °C, SS 316L exhibits the highest stress of all the alloys to date, with a stress of 240.5 MPa, confirming that the CTE is the major contributor to low to intermediate-stress levels during thermal cycling when all alloy E(T) values are still close together.

This finding has significant ramifications for engineering design: Because components made from SS 316L in thermally restrained assemblies will experience much greater thermal stresses than components made from Ni-based superalloys, extensive thermal compliance design must occur to avoid liquid stress failure at ambient pressure inside pipes, pressure vessels, heat exchangers, etc., made from SS 316L.

The thermal stress produced by Inconel 718 was the next-highest at 1225 MPa at 600 degrees Celsius (°C). The primary cause of the elevated thermal-stress response of Inconel 718 is its relatively high modulus of elasticity (E). There is also a small contribution from the CTE (Coefficient of Thermal Expansion) of the material. At 600 °C, Inconel 718 has a CTE of 13 x 10⁻⁶/°C; This is moderate compared to the elevated E(T), which varies between 200 and159 GPa (depending on temperature). At 300 °C, Inconel 718 has a thermal stress level of 665 MPa compared to 582.9 MPa for Hastelloy C276 despite Hastelloy C276's higher absolute modulus at that temperature. Inconel 718's overall higher CTE was the main reason for its thermal stress difference (13 vs.11.2 x 10⁻⁶/°C). Thus, it can be concluded that thermal stress does not just depend on stiffness in constrained systems; the interaction between E and CTE (E·CTE) for a

particular material/application combination also has a significant effect on the amount of thermal stress generated in constrained materials.

Hastelloy C276 has a moderate thermal stress of 1061 MPa at 600 °C - the third highest of all five alloy materials, but it is much lower than either type of717L or Inconel718, whilst having the highest initial elastic modulus (205 GPa at 20°C). The difference of C276 being the lowest CTE out of all five/alloy materials (α=11.2 x 10^{-6}/°C) compensates for its high modulus in the E·α products due to this thermomechanical property of C276 allowing it to provide advantages when using multiple material assemblies, where differences in thermal expansion between materials at interfaces must be minimized by its high structural rigidity (stiffness) providing structural support while at the same time providing a low CTE limiting thermal strain between adjacent metals through the direct correlation to its common use as a chemical reactor internal component, heat exchanger tube sheet assembly and nuclear containment facility.

Cu C110 produced thermal stress of 893.6 MPa at 600°C, the fourth highest of all the alloys, due to its high CTE (a = 17 × 10^{-6} /°C, the highest out of the 5) but low elastic modulus (90 GPa at 600°C) partially offsets this. The net E·α product from Cu C110 is lower than that of the Ni-based alloys and SS 316L resulting in lower amounts of thermal stress generated although Cu C110 has an advantage in CTE. Although Cu C110 has a high thermal stress level at elevated temperatures and relatively low strength, from an engineering point of view, Cu C110 is not an appropriate material for constrained structural applications above 300 °C. At this temperature, σ_Cu reaches 497.6 MPa, which is close to the yield strength of annealed cu alloys.

In terms of thermal stress, Ti-6Al-4V exhibited the lowest levels across all five alloys for the full range of temperature. At 600 °C, Ti-6Al-4V generated 442.1 MPa of thermal stress, which was less than one-third of SS 316L's value at the same temperature. The outstanding thermal stress response of Ti-6Al-4V at elevated temperatures is mainly a consequence of its low coefficient of thermal expansion (CTE) (α = 8.6×10^{-6} /°C, the lowest of all five alloys) and its lower elastic modulus, leading to a very small E·α product compared to the other four alloys. As a result, Ti-6Al-4V produces minimal constrained thermal stress during elevated temperature service; this property is especially important in aerospace structures, where Ti-6Al-4V is often used in conjunction with dissimilar materials (composites, aluminum alloys, steels), and the thermomechanical compatibility of the interface between dissimilar materials strongly influences joint integrity and fatigue life.

Table 8. Thermal stress σ (MPa) at selected temperatures for five metallic alloys.

T (°C)	Cu C110	Ti-6Al-4V	Inconel 718	Hastelloy C276	SS 316L
20	0	0	0	0	0
100	154.0	75.97	202.7	178.7	240.5
200	333.4	164.5	442.1	388.7	523.1
300	497.6	245.7	665.0	582.9	783.8
400	646.1	319.2	870.5	760.2	1021
500	778.3	384.8	1057	919.9	1232
600	**893.6**	**442.1**	**1225**	**1061**	**1415**

4.5.4 The E·α Product — Governing Parameter for Thermal Stress Ranking

Thermal stress analysis shows that there isn't any correlation between how the alloys rank based on stress; however, all five alloys are ranked based on the product E·α which includes both of the previous rankings. A graphical representation of each alloy's ranking at 300 degrees Celsius can be seen in Table 7. Consistently across the entire temperature range of operating conditions, the E·α ranking (SS 316L > Inconel 718 > Hastelloy C276 > Cu C110 > Ti-6Al-4V) confirms once again that the composite parameter is the main predictor of thermal stress in constrained metallic

alloys. This knowledge provides a quantitative basis for selecting materials for thermally constrained engineering applications; if thermal stress is the principal mode of failure, the governing design factor to minimize is E·α.

Table 9. Composite thermomechanical parameter E·α at T = 300 °C.

Alloy	E at 300°C (GPa)	α (×10⁻⁶/°C)	E·α (MPa/°C)	σ at 300°C (MPa)
SS 316L	176.0	16.0	2.816	783.8
Inconel 718	183.0	13.0	2.379	665.0
Hastelloy C276	186.0	11.2	2.083	582.9
Cu C110	105.0	17.0	1.785	497.6
Ti-6Al-4V	103.0	8.6	0.886	245.7

4.5.5 Engineering Implications and Design Recommendations

Four recommendations can be made based on the analyses of temperatures and thermal stresses in both Figure 8 and Tables 8-9 as follows:

1. Thermal stress awareness: At a temperature of 300 °C, the thermal stress that results in SS 316L and Inconel 718 is already 783.8 MPa and 665.0 MPa, respectively, and this approaches the elevated-temperature yield strength of these alloys (depending on the condition of treatment). Therefore, it is imperative to verify that σ_thermal < σ_yield (T) for elastic safety when designing component parts that will be subjected to cyclic loads or subjected to creating thermal ratcheting or low cycle fatigue.
2. Ti-6Al-4V is the optimal material for thermo mechanical compatibility: The E·α product for the Ti-6Al-4V alloy (0.886 MPa/°C) at 300 °C is less than 1/3 the next lowest alloy (Cu C110, 1.785 MPa/°C). Therefore, Ti-6Al-4V is an excellent choice for thermomechanical compatibility within constrained multi-material assemblies (i.e., aerospace and biomedical structural joints).
3. Hastelloy C276 is the best combination of stiffness, thermal stress: Hastelloy C276 has the highest initial stiffness of all test materials; however, Hastelloy C276's low CTE (11.2×10⁻⁶ /°C) provides an intermediate E·α(2.083 MPa/°C). Thus, Hastelloy C276 is used when both high stiffness and controlled thermal stresses are needed (i.e., on reactor pressure boundary and nuclear heat exchanger components).
4. SS 316L requires thermal stress management: SS 316L's highest E·α product (2.816 MPa/°C) at 300 °C requires specific thermal stress management strategies (i.e., expansion loops, bellows, etc.) in any structural application with constraints and temperatures over 200 °C.

4.6 Material Selection Framework and Final Ranking

4.6.1 Multi-Criteria Evaluation

When choosing materials for demanding thermal applications, multiple competing requirements need to be assessed simultaneously. Four numerical performance metrics based on Sections 4.1–4.5 will be combined to provide a basis for material selection: absolute elastic modulus E(T), retention loss, thermal sensitivity |dE/dT|, and thermal stress σ(T). The four metrics are combined into one table, Table 8, that lists the primary performance values for each material of interest (i.e., 600°C) throughout the alloy selection.

Table 10. Thermomechanical performance summary at 600 °C.

Alloy	E (GPa)	Retention Loss (%)	|dE/dT| (GPa/°C)	σ (MPa)
Cu C110	90	22.28	0.04804	893.6

Ti-6Al-4V	88	22.02	0.04638	442.1
Inconel 718	159	18.59	0.07128	1225
Hastelloy C276	159	20.16	0.07963	1061
SS 316L	151	20.84	0.08135	1415

4.6.2 Weighted Scoring and Final Ranking

All metrics are scaled from 1 to 5 in relation to their structural priority; the lower number indicates lower performance. The following table shows all ratings along with final composite scores. The overall ranking by materials is as follows; Inconel 718—1st; Hastelloy C276—2nd; Ti-6Al-4V—3rd; Cu C110—4th; SS 316L—5th. Inconel 718 received the highest composite score due to its superior loss of stiffness (18.59% at 600 °C) and highest absolute modulus due to its stable γ'/γ" precipitation-hardened microstructure. Hastelloy C276 received second place due to having the highest ambient (>205 GPa) and lowest coefficient of thermal expansion (CTE = 11.2×10^{-6} /°C) among the four candidates giving it greater resistance to thermal stress despite having a greater initial stiffness than Inconel 718. Ti-6Al-4V, ranked third, has a low E·α product (0.886 MPa/°C at 300 °C) creating less than one-third of the thermal stress created by SS316L at 600 °C therefore making it the best candidate for thermomechanical compatibility in weight sensitive and multi-material constrained assemblies. SS 316L ranked last; therefore its moderate stiffness resulted in the highest thermal stress (1415 MPa) and sensitivity (0.08135 GPa/°C) at 600 °C, limiting this material's use to applications at or below 300 °C where the corrosion resistance and weldability provide significant advantages. See Table 11.

Table 11. Normalized scoring matrix and final ranking at 600 °C.

Criterion	Weight	Cu C110	Ti-6Al-4V	Inconel 718	Hastelloy C276	SS 316L
E(T)	30%	1	1	5	5	4
Retention	25%	1	2	5	4	3
|dE/dT|	20%	5	5	3	2	1
σ_thermal	25%	3	5	2	3	1
Score		**2.35**	**3.20**	**3.85**	**3.70**	**2.30**

4.6.3 Temperature-Specific Recommendations

The optimal material selection is inherently temperature-dependent. Table 12 provides application-specific guidance across the full investigated thermal range:

Table 12. Application-specific material selection guidance.

Temperature Range	Recommended Alloy	Rationale
20–200 °C	Hastelloy C276	Highest absolute stiffness
200–600 °C	Inconel 718	Best retention + stable microstructure
All ranges (low weight)	Ti-6Al-4V	Best specific stiffness E/ρ
All ranges (low σ)	Ti-6Al-4V	Lowest E·α product
Corrosive environments	Hastelloy C276	Corrosion + stiffness
Cost-sensitive < 300°C	SS 316L	Availability + moderate performance

4.6.4 Limitations and Future Work

The current multi-criteria decision support framework uses an equal weighting approach for each temperature range. In addition, there are fixed weights assigned to each criterion

(30/25/20/25%), which are based on generic priorities in structural design. In practice, this approach may produce a different ranking based on application-specific weighting schemes. For instance, in a corrosion-dominated environment, Hastelloy C276 will be ranked higher than it would normally be because of its additional weight for chemical resistance. Finally, the current analysis assumes that coefficients of thermal expansion (CTE) for all alloys are constant, while experimental data for CTE show some mild increase with temperature, particularly with Ti-6Al-4V beyond 400 °C; thus, this may slightly affect the thermal stress calculations at the upper thermal boundary. Future studies must take into consideration temperature dependent CTE data sets and expand the simulation framework to operate at higher temperatures (600–1000 °C), to obtain all of the service conditions needed for Ni-based superalloys and to understand the α→β transformation phase for Ti-6Al-4V.

5. Conclusions

This work developed and validated a dual method EES-based simulation platform to estimate the temperature-dependent elastic modulus and select materials for five engineering metallic alloys between 20 and 600 °C. The membership of main conclusions is as follows:

- The second-order polynomial regression model (Method B) adequately emulated the experimental reference data (Method A) with maximum cross-validation error of 2.70% for Inconel 718 and Hastelloy C276 at 600 °C, with the minimum recorded error being 0% at the lower thermal boundary for all alloys. Sub-3% accuracy was attained across the thermal range, and this establishes the engineering credibility of the polynomial regression procedure as a computationally inexpensive alternative to tabular data interpolation in thermomechanical simulation workflows.
- The five alloys all exhibited a continuous loss in the moderate and non-linear behaviour of their elastic modulus with increasing temperature, resulting in an average loss of 21.3% at 600 °C. The order of elastic modulus from highest to lowest was the same at all heating regimes; it was found to be Hastelloy C276 ≥ Inconel 718 > Stainless Steel 316L >> Copper C110 ~ Titanium-6Al-4V. The consistent behavior across the complete thermal regime of all five alloys provides evidence that alloy chemistry and microstructure based mechanisms of strengthening have a primary role in their respective comparative elastic stiffnesses under thermal loads.
- The analysis for the elastic modulus retention loss, Inconel 718, was the most thermally stable alloy (18.59% loss at 600 °C), due to the coherent γ'/γ" precipitation hardening microstructure. The maximum amount of relative degradation was Cu C110 with 22.28% total loss, which is attributed to its pure FCC lattice structure and lack of any form of microstructure stabilization mechanism.
- The analysis of thermal sensitivity between the five alloys from 20-600 °C demonstrated a consistent bifurcation into two separate groups; the low sensitivity group included Copper C110 with $|dE/dT|$ = 0.04804 GPa/°C at 600 °C and Titanium-6Al-4V with $|dE/dT|$ = 0.04638 GPa/°C, and the high sensitivity group included Stainless Steel 316L with $|dE/dT|$ = 0.08135 GPa/°C, Hastelloy C276 with $|dE/dT|$ = 0.07963 GPa/°C and, Inconel 718 with $|dE/dT|$ = 0.07128 GPa/°C. This classification provides direct guidance as to the types of alloys that are most likely to perform well in thermally cyclic and transient loads.
- The analysis of thermal stress showed that constrained thermal stress formation is determined by E·α composite parameter rather than simply elastic modulus or thermal expansion coefficient; therefore wire having an E·α composite parameter value > 2.815 MPa/°C will produce more than one-third of the maximum possible thermal stress (E·α = 0.886 MPa/°C) at higher temperatures (600 °C) than a wire with an E·α composite parameter value < 2.815 MPa/°C. This is supported by experimental data that show SS 316L produces the maximum thermal stress (1415 MPa when E·α = 2.816 MPa/°C at 300 °C), while Ti-6Al-4V produces the least thermal stress (442.1 MPa at 600 °C E·α = 0.886 MPa/°C) therefore, Ti-6Al-4V can

be considered to be the best alloy for high-utility use in thermomechanically compatible constrained multi-material assemblies.

- The multi-criteria material selection process results indicate the final composite ranking: Inconel 718 (3.85) > Hastelloy C276 (3.70) > Ti-6Al-4V (3.20) > Copper 110 (2.35) > SS 316L (2.30). The recommended primary structural alloy for high temperature (200–600 °C) applications requiring optimal stiffness retention is Inconel 718 while for those applications where thermomechanical compatibility and specific stiffness dictate design, the preferred alloy is Ti-6Al-4V. For corrosion critical/ at high-temperature (≤ 600 °C) applications the Inconel 718 is the best wire due to its balance compression of absolute stiffness with controlled thermal stress, while SS 316L remains cost effective when used in applications ≤ 300 °C.
- The developed EES framework can calculate the full thermal elasticity of a material (alloy) using 3 scalar polynomial coefficients (a,b,c). The direct calculation of E(T) and dE/dT at any temperature in the validated range is possible, without needing to use various methods of interpolation. This will also integrate easily into digital twin, FEA, and material selection algorithms for engineers using materials subject to high thermal loads.

References

[1] E. Isotta, W. Peng, A. Balodhi, and A. Zevalkink, "Elastic Moduli: a Tool for Understanding Chemical Bonding and Thermal Transport in Thermoelectric Materials," Mar. 13, 2023, *John Wiley and Sons Inc*. doi: 10.1002/anie.202213649.

[2] B. Rehmer, F. Bayram, L. A. Ávila Calderón, G. Mohr, and B. Skrotzki, "Elastic modulus data for additively and conventionally manufactured variants of Ti-6Al-4V, IN718 and AISI 316 L," *Sci. Data*, vol. 10, no. 1, Dec. 2023, doi: 10.1038/s41597-023-02387-6.

[3] W. Li *et al.*, "Temperature-dependent elastic modulus model for metallic bulk materials," *Mechanics of Materials*, vol. 139, p. 103194, May 2019, doi: 10.1016/j.mechmat.2019.103194.

[4] Z. Kong *et al.*, "Mechanical properties of SLM 316L stainless steel plate before and after exposure to elevated temperature," *Constr. Build. Mater.*, vol. 444, p. 137786, 2024, doi: https://doi.org/10.1016/j.conbuildmat.2024.137786.

[5] C. Jin *et al.*, "High-throughput calculation integrated with stacking ensemble machine learning for predicting elastic properties of refractory multi-principal element alloys," *Materials Genome Engineering Advances*, vol. 3, no. 3, Sep. 2025, doi: 10.1002/mgea.70004.

[6] ASM International, "ASM Handbook: Properties and Selection: Nonferrous Alloys and Special-Purpose Materials.," vol. 2, 2019.

[7] *MMPDS-14 : metallic materials properties development and standardization (MMPDS). Chapters 1-9.* District of Columbia, United States: [Washington, D.C.] : Federal Aviation Administration ; [Columbus, Ohio] : Battelle Memorial Institute, 2019. [Online]. Available: https://searchworks.stanford.edu/view/13856199

[8] Haynes International, "Hastelloy C-276 Alloy Technical Bulletin," 2023.

[9] S. M. A. A. Alvi, J. Janssen, D. Khatamsaz, D. Perez, D. Allaire, and R. Arróyave, "Hierarchical Gaussian process-based Bayesian optimization for materials discovery in high entropy alloy spaces," *Acta Mater.*, vol. 289, p. 120908, 2025, doi: https://doi.org/10.1016/j.actamat.2025.120908.

[10] K. Guo, Z. Yang, C. H. Yu, and M. J. Buehler, "Artificial intelligence and machine learning in design of mechanical materials," Apr. 01, 2021, *Royal Society of Chemistry*. doi: 10.1039/d0mh01451f.

[11] L. Yu, J. Zhai, W. Cao, and J. Ren, "Prediction of temperature-dependent yield strength of refractory high entropy alloy based on stacking integrated framework," *Journal of materials Informatics*, vol. 4, no. 4, Dec. 2024, doi: 10.20517/jmi.2024.39.

[12] H. Khakurel *et al.*, "Machine learning assisted prediction of the Young's modulus of compositionally complex alloys," *Sci. Rep.*, vol. 11, no. 1, Dec. 2021, doi: 10.1038/s41598-021-96507-0.
[13] J. Peng, Y. Yamamoto, J. A. Hawk, E. Lara-Curzio, and D. Shin, "Coupling physics in machine learning to predict properties of high-temperatures alloys," *NPJ Comput. Mater.*, vol. 6, no. 1, Dec. 2020, doi: 10.1038/s41524-020-00407-2.
[14] S. Liu, K. Lee, and P. V Balachandran, "Integrating machine learning with mechanistic models for predicting the yield strength of high entropy alloys," *J. Appl. Phys.*, vol. 132, no. 10, p. 105105, Sep. 2022, doi: 10.1063/5.0106124.
[15] A. Mishra, "LatticeML: a data-driven application for predicting the effective Young Modulus of high temperature graph based architected materials," *International Journal on Interactive Design and Manufacturing (IJIDeM)*, vol. 19, no. 5, pp. 3899–3920, 2025, doi: 10.1007/s12008-024-01976-y.
[16] G. Ouyang *et al.*, "Design of refractory multi-principal-element alloys for high-temperature applications," *NPJ Comput. Mater.*, vol. 9, no. 1, Dec. 2023, doi: 10.1038/s41524-023-01095-4.
[17] L. Rickard, A. Bampoulas, M. Laad, and E. Mangina, "AI-driven optimisation of metal alloys for space applications," *Discover Artificial Intelligence*, vol. 5, no. 1, Dec. 2025, doi: 10.1007/s44163-025-00260-6.
[18] H. Zhang *et al.*, "Dramatically Enhanced Combination of Ultimate Tensile Strength and Electric Conductivity of Alloys via Machine Learning Screening," *Acta Mater.*, vol. 200, pp. 803–810, 2020, doi: https://doi.org/10.1016/j.actamat.2020.09.068.
[19] D. Khatamsaz, B. Vela, P. Singh, D. D. Johnson, D. Allaire, and R. Arróyave, "Bayesian optimization with active learning of design constraints using an entropy-based approach," *NPJ Comput. Mater.*, vol. 9, no. 1, p. 49, 2023, doi: 10.1038/s41524-023-01006-7.
[20] S. A. Giles, D. Sengupta, S. R. Broderick, and K. Rajan, "Machine-learning-based intelligent framework for discovering refractory high-entropy alloys with improved high-temperature yield strength," *NPJ Comput. Mater.*, vol. 8, no. 1, p. 235, 2022, doi: 10.1038/s41524-022-00926-0.
[21] S. Risal, N. Singh, Y. Yao, L. Sun, S. Risal, and W. Zhu, "Accelerating Elastic Property Prediction in Fe-C Alloys through Coupling of Molecular Dynamics and Machine Learning," *Materials*, vol. 17, no. 3, Feb. 2024, doi: 10.3390/ma17030601.
[22] Cao J *et al.*, "Intelligent Design and Simulation of High-Entropy Alloys via Machine Learning and Multiobjective Optimization Algorithms," *J Chem Theory Comput.*, vol. 14, no. 21, pp. 7051–7061, 2025, doi: 0.1021/acs.jctc.5c00143.
[23] A. Balan *et al.*, "Precipitation of γ in Inconel 718 alloy from microstructure to mechanical properties," *SSRN Electronic Journal*, 2021, doi: 10.1016/j.jmrt.2021.xx.
[24] Z. Qiu *et al.*, "Effects of post heat treatment on the microstructure and mechanical properties of wire arc additively manufactured Hastelloy C276 alloy," *Mater. Charact.*, vol. 177, p. 111158, May 2021, doi: 10.1016/j.matchar.2021.111158.
[25] Z. Kong *et al.*, "Mechanical properties of SLM 316L stainless steel plate before and after exposure to elevated temperature," *Constr. Build. Mater.*, vol. 444, p. 137786, 2024, doi: https://doi.org/10.1016/j.conbuildmat.2024.137786.
[26] G. Lütjering and J. Williams, *Titanium*. 2007. doi: 10.1007/978-3-540-73036-1.
[27] B. Ni, B. Glaser, and S. M. Taheri-Mousavi, "End-to-end prediction and design of additively manufacturable alloys using a generative AlloyGPT model," *NPJ Comput. Mater.*, vol. 11, no. 1, Dec. 2025, doi: 10.1038/s41524-025-01768-2.
[28] P. Liu *et al.*, "Machine learning assisted design of γ′-strengthened Co-base superalloys with multi-performance optimization," *NPJ Comput. Mater.*, vol. 6, no. 1, Dec. 2020, doi: 10.1038/s41524-020-0334-5.
[29] M. Dai *et al.*, "Accelerated Design of Mechanically Hard Magnetically Soft High-entropy Alloys via Multi-objective Bayesian Optimization," 2026.

[30] H.-G. Nguyen, T.-D. Le, H.-G. Nguyen, and T.-H. Fang, "Mechanical properties of AlCoCrCuFeNi high-entropy alloys using molecular dynamics and machine learning," *Materials Science and Engineering: R: Reports*, vol. 160, p. 100833, 2024, doi: https://doi.org/10.1016/j.mser.2024.100833.
[31] B. Steingrimsson, X. Fan, X. Yang, M. C. Gao, Y. Zhang, and P. K. Liaw, "Predicting temperature-dependent ultimate strengths of body-centered-cubic (BCC) high-entropy alloys," *NPJ Comput. Mater.*, vol. 7, no. 1, Dec. 2021, doi: 10.1038/s41524-021-00623-4.
[32] F. Rousseau, T. Belmonte, F. Sur, and A. Nominé, "Inverse Design of High-Entropy Superalloys Using Machine Learning and Generative Artificial Intelligence," Dec. 25, 2025. doi: 10.21203/rs.3.rs-8393509/v1.
[33] Z. Li and N. Birbilis, "Multi-objective Optimization-Oriented Generative Adversarial Design for Multi-principal Element Alloys," *Integr. Mater. Manuf. Innov.*, vol. 13, no. 2, pp. 435–444, Jun. 2024, doi: 10.1007/s40192-024-00354-6.
[34] L. Zhichao, M. Dong, L. Xiongjun, and Z. Lu, "High-throughput and data-driven machine learning techniques for discovering high-entropy alloys," Dec. 01, 2024, *Springer Nature*. doi: 10.1038/s43246-024-00487-3.
[35] X. Wan *et al.*, "Machine Learning Paves the Way for High Entropy Compounds Exploration: Challenges, Progress, and Outlook," *Advanced Materials*, vol. 37, no. 31, p. 2305192, Aug. 2025, doi: https://doi.org/10.1002/adma.202305192.
[36] G. Vazquez, D. Sauceda, and R. Arróyave, "Deciphering chemical ordering in High Entropy Materials: A machine learning-accelerated high-throughput cluster expansion approach," *Acta Mater.*, vol. 276, p. 120137, 2024, doi: https://doi.org/10.1016/j.actamat.2024.120137.
[37] B. Mortazavi, "Recent Advances in Machine Learning-Assisted Multiscale Design of Energy Materials," *Adv. Energy Mater.*, vol. 15, no. 9, p. 2403876, Mar. 2025, doi: https://doi.org/10.1002/aenm.202403876.
[38] B. Guomundsson and G. Lorna, "Automated Design Using Machine Learning in Materials Engineering - An Explicit Forecasts," *Journal of Computational Intelligence in Materials Science*, pp. 56–66, May 2023, doi: 10.53759/832x/jcims202301006.
[39] X. Tan *et al.*, "Machine learning and high-throughput computational guided development of high temperature oxidation-resisting Ni-Co-Cr-Al-Fe based high-entropy alloys," *NPJ Comput. Mater.*, vol. 11, no. 1, Dec. 2025, doi: 10.1038/s41524-025-01568-8.
[40] D. Shin, Y. Yamamoto, M. P. Brady, S. Lee, and J. A. Haynes, "Modern data analytics approach to predict creep of high-temperature alloys," *Acta Mater.*, vol. 168, pp. 321–330, 2019, doi: https://doi.org/10.1016/j.actamat.2019.02.017.
[41] N. Li, C. Wang, and C. Li, "Microstructures and High-Temperature Mechanical Properties of Inconel 718 Superalloy Fabricated via Laser Powder Bed Fusion," *Materials*, vol. 17, no. 15, Aug. 2024, doi: 10.3390/ma17153735.
[42] P. Mohazzabi, "Temperature dependence of the elastic constants of copper, gold and silver," *Journal of Physics and Chemistry of Solids*, vol. 46, pp. 147–150, 1985, [Online]. Available: https://api.semanticscholar.org/CorpusID:95051357